

CONFERENCES AND SYMPOSIA

PACS numbers: 61.20.Gy, 61.20.Ne, 64.60.Kw

Physics of phase transitions in two dimensions: Berezinskii–Kosterlitz–Thouless and beyond *

V.N. Ryzhov, V.V. Brazhkin, E.E. Tareyeva, Yu.D. Fomin, E.N. Tsiok

DOI: https://doi.org/10.3367/UFNe.2025.04.040000

Contents

Abstract. This review is based on the authors' report at the Scientific Session of the Physical Sciences Division of the Russian Academy of Sciences (RAS). The review discusses the Berezinskii–Kosterlitz–Thouless (BKT) transition in two-dimensional systems with continuous symmetry, including the transition in two-dimensional magnetic systems ($X-Y$-model), the transition to the superfluid state in ^{4}He thin films, and the superconducting transition in thin films. Scenarios of two-dimensional melting in various systems are considered, including soft matter, vortex lattices in superconducting films, and skyrmion lattices. Particular attention is paid to deviations from the standard BKT scenario for various systems depending on the parameters characterizing the system: the type of potential, which is especially important for two-dimensional melting, and the energy of the core of a topological defect.

Keywords: two-dimensional systems, Berezinskii–Kosterlitz–Thouless transition, superfluid films, superconducting films, $X-Y$-model, two-dimensional crystals, topological defects, vortices, dislocations, disclinations, hexatic phase, two-dimensional melting, Berezinskii–Kosterlitz–Thouless–Halperin–Nelson–Young theory, first order transition, Bernard–Krauth scenario

V.N. Ryzhov [a], **V.V. Brazhkin** [b], **E.E. Tareyeva** [c], **Yu.D. Fomin** [d], **E.N. Tsiok** [e]
Vereshchagin Institute for High Pressure Physics,
Russian Academy of Sciences,
Kaluzhskoe shosse 14, 108840 Troitsk, Moscow, Russian Federation
E-mail: [a] ryzhov@hppi.troitsk.ru, [b] brazhkin@hppi.troitsk.ru,
[c] etare@ms2.inr.ac.ru, [d] fomin314@mail.ru,
[e] elena.tsiok@gmail.com

Received 18 July 2025
Uspekhi Fizicheskikh Nauk **196** (5) 537 – 561 (2026)
Translated by the authors

1. Introduction

Phase transitions constitute one of the most widespread and remarkable phenomena encountered both in everyday life and in fundamental research and technological applications. A theory that proved to be capable of describing the fundamental aspects of the physics of phase transitions was proposed by L.D. Landau in 1937 [1]. The Landau theory of phase transitions stands as one of the fundamental approaches to describing critical phenomena in systems undergoing phase transitions. At its core lie the concept of an order parameter — a macroscopic quantity that characterizes the degree of ordering in a system — and the analysis of the free energy as a function of this parameter. By employing the methods of thermodynamics and symmetry analysis, Landau proposed a universal formalism, which allows one to classify phase transitions and to predict their fundamental properties. The central point of Landau's theory is the concept of an order parameter that he introduced — a quantity equal to zero above the transition temperature in the disordered phase and becoming nonzero upon transition to the ordered phase. The order parameter characterizes the symmetry breaking that occurs during a phase transition. Phase transitions, according to the standard classification, are of two types: first-order transitions, where the order parameter changes discontinuously, and continuous transitions (often referred to as second-order transitions), in which the order parameter varies continuously. The simplest example of an order parameter is the magnetization (average value of the magnetic moment) in a ferromagnet. At a qualitative level, the transition in a magnet can be

* This review is based on the report presented for the Scientific Session of the Physical Sciences Division of the Russian Academy of Sciences (PSD RAS), on April 23, 2025 (see *Physics–Uspekhi* **69** (5) 419 (2026); *Uspekhi Fizicheskikh Nauk* **196** (5) 449 (2025)).

represented as follows: at high temperatures, the magnetic moments rotate freely, while the system is isotropic, i.e., there is no preferred direction in it. However, upon lowering the temperature, at a certain critical value of temperature T_c, the system exhibits a spontaneous appearance of a nonzero value of magnetization (the order parameter), i.e., a phase transition into the ferromagnetic state occurs with the appearance of the preferred direction, which coincides with the direction of the magnetization vector — i.e., the system ceases to be isotropic.

Despite its simplicity and phenomenological character, the Landau theory has had a profound impact on the development of statistical physics and condensed matter theory. It successfully describes second-order transitions in a broad range of systems: from ferromagnets and superconductors to liquid crystals and structural phase transformations in solids. The most remarkable accomplishment of this theory was the phenomenological description of superconductivity, recognized with the Nobel Prize awarded to A.A. Abrikosov and V.L. Ginzburg in 2003. At the same time, by the 1960s it had become clear that taking fluctuations into account is crucial for a correct description of the behavior of a system in the vicinity of a second-order phase transition. All this led to the creation of the fluctuation theory of phase transitions (A.Z. Patashinsky, V.L. Pokrovsky, L. Kadanoff, M. Fisher, K. Wilson) (see, e.g., [2–10]). At the same time, theoretical studies demonstrated that the dimensionality of space is of fundamental importance in the physics of phase transitions. In particular, for the de facto basic model, which is extensively used to describe phase transitions in magnetic systems — the Ising model with short-range interactions (see, e.g., [9, 10, 23]) — it was found that the phase transition is absent in one dimension, and the transition parameters differ significantly, in particular the behavior of the order parameter in the vicinity of the transition temperature for two and three dimensions.

The symmetry of the order parameter is also of fundamental importance. In particular, the works of Landau [1], Peierls [11, 12], and later Bogoliubov, Mermin, and Wagner [24–28] demonstrated that in two-dimensional systems with a continuous symmetry of the order parameter — such as the Heisenberg magnet, the X–Y model, superfluid and superconducting systems, as well as two-dimensional crystal lattices — thermal fluctuations become infinitely large and destroy long-range order.

To demonstrate this, we shall consider the behavior of the correlation function of order-parameter fluctuations in degenerate planar systems [9]. Thermodynamic potential of transverse fluctuations of the order parameter $\boldsymbol{\varphi}_\perp$ can be written as:

$$\Phi_\perp = \frac{1}{2}\int \left(\frac{h}{\varphi}\, \boldsymbol{\varphi}_\perp^2 + J\,(\nabla \boldsymbol{\varphi}_\perp)^2 \right) \mathrm{d}^d r\,. \tag{1}$$

where h is the external field and d is the dimensionality of space. The mean-square fluctuation of the Fourier transform of the order parameter takes the form:

$$\left\langle |\boldsymbol{\varphi}_\perp(q)|^2 \right\rangle = \frac{T}{h/\varphi + Jq^2}\,. \tag{2}$$

The mean-square fluctuation of the order parameter at a given point can be written as:

$$\left\langle \boldsymbol{\varphi}_\perp^2(\mathbf{r}) \right\rangle = \frac{T}{(2\pi)^d}\int \frac{d^d q}{h/\varphi + Jq^2}\,. \tag{3}$$

From equation (3) one can see that, at $h = 0$, transverse fluctuations become infinitely large at $d = 1, 2$ but remain finite in the case of three dimensions. The contradiction can be resolved by assuming that $\varphi \to 0$ as $h \to 0$, leading to the conclusion that in systems with $d = 1$ and $d = 2$ dimensionality long-range order is absent at $T \neq 0$.

From this it followed that in such systems phase transitions are possible only at zero temperature. At the same time, experimental studies on superfluidity in thin films of liquid ^{4}He [29–35] appeared, as well as a number of studies based on computer modeling of hard disks [36–39] and numerical methods applied to magnetic systems [40–42] — their results contradicted the aforementioned conclusion.

Clarity on these issues was provided in the works of Berezinskii, Kosterlitz, and Thouless [13–15, 43, 44]. It turned out that, despite the absence of long-range order, two-dimensional magnets resist nonuniform spin rotation, and a thin film of liquid helium at low temperatures exhibits the property of superfluidity. Two-dimensional crystals, despite the absence of long-range translational order, have a finite shear modulus, i.e., they are solids. Berezinskii grasped the general nature of these phenomena and gave them the name transverse rigidity, now commonly employed in the scientific literature worldwide.

He showed that in systems with transverse rigidity the correlation functions of the order parameter slowly, according to a power law, decrease with distance, while the value of exponent depends on the interaction parameters and temperature. This new phase, which is sometimes referred to as the Berezinskii phase, possesses quasi-long-range order. Since, in the high-temperature disordered phase, correlations decay exponentially quickly, one can conclude that at a certain temperature a phase transition occurs, in which the asymptotic behavior of the correlation functions changes.

Berezinskii [13, 14] was the first to discover the important role of topological defects upon transition: vortices in a superfluid helium film, dislocations in a two-dimensional crystal, vortex configurations in a two-dimensional magnet with two-component magnetic moments (the X–Y model); he also gave a qualitative explanation of the transition mechanism. At low temperatures, the defects form bound pairs that do not destroy the quasi-long-range order. However, as the temperature increases, dissociation of bound pairs occurs, and free defects appear which transform the quasi-long-range order into a disordered phase with a rapid exponential decrease in correlations. The method for calculating the transition temperature was developed in subsequent works by Kosterlitz and Thouless [15, 43, 44].

More than 50 years after the seminal works of Berezinskii [13, 14] and Kosterlitz and Thouless [15, 16], the Berezinskii–Kosterlitz–Thouless (BKT) transition remains one of the most relevant examples of topological phase transitions in condensed matter systems and continues to be the subject of intensive experimental and theoretical research. This transition, associated with topological defects in two-dimensional systems, opened new horizons in the understanding of phenomena occurring in two-dimensional and quasi-two-dimensional systems, such as superfluidity in thin films, two-dimensional magnets, thin superconducting films, and even high-temperature superconductors.

Several systems fall into the universality class of the BKT transition, including a one-dimensional electron system exhibiting a quantum metal–insulator transition, a two-dimensional Coulomb gas, and, of course, superfluid and

superconducting systems in two dimensions [16–18, 22, 45, 46]. The transition to the superfluid state has been investigated in neutral superfluid liquids, such as thin films of ^{4}He [47–49] and systems of ultracold atoms in optomagnetic traps, consisting of bosons [50] or neutral fermions [51]. It should be noted that it was the experiments on detecting the BKT transition in thin ^{4}He films [47, 49] that triggered an avalanche of interest in this problem. Nevertheless, despite the fact that in the original article by Kosterlitz and Thouless [15] the authors asserted that the BKT transition should not be observed in (quasi-)two-dimensional superconductors, this is certainly the area where it is most widely discussed. Although the conditions under which BKT physics can be observed in quasi-two-dimensional superconductors are not always satisfied, the ideas underlying the BKT transition are actively used to provide approximate explanations for phenomena observed in a wide class of systems: thin films of conventional [84, 85, 87, 88, 91, 99 – 109] and unconventional [110–112] superconductors, as well as in two-dimensional electron gases formed at the interface between two insulators in artificial heterostructures [113–115] or in the top layer of ion-gated superconducting systems [116].

The BKT theory appears to be universal and relevant to all two-dimensional systems with continuous symmetry. However, there are a number of problems where further development of the theory is required for a correct description of the experimental situation. For example, experiments [88, 102–104] clearly show that as the film thickness decreases, the temperature dependence of the superconducting electron density begins to deviate sharply from the corresponding dependence dictated by the Bardeen–Cooper–Schrieffer (BCS) theory. However, this deviation appears to occur at a temperature lower than that predicted by the standard expression for the BKT transition temperature, which calls into question the universality of the relation between the superfluid density and the critical temperature — one of the hallmarks of the BKT transition. Furthermore, the interaction between vortices in the X–Y model and in a thin ^{4}He film differs significantly from the vortex interaction in a thin superconducting film, which means that the BKT theory can only be approximately applied to describe the transition in this system.

Even more striking deviations from the standard BKT theory occur in the theory of two-dimensional melting. The theory of two-dimensional melting, developed in the late 1970s in the famous works of Halperin, Nelson, and Young [17–19, 52–54], is a separate and very important branch of BKT theory. In these works, it was shown that, unlike the case of three dimensions, where melting always occurs via a single first-order transition, in two dimensions the system can melt via two continuous BKT-type transitions with an intermediate hexatic (orientationally ordered) phase between the crystal and the isotropic liquid. The reason for this is the strongly developed fluctuations in two-dimensional systems. This theory is usually called the Berezinskii–Kosterlitz-Thouless–Halperin–Nelson–Young (BKTHNY) theory. The emergence of BKTHNY theory led to a huge number of experimental and theoretical works, as well as computer simulations of various two-dimensional systems aimed at testing it. This led to the understanding that, in addition to the BKTHNY scenario, there are two others, which will also be discussed below, in which melting can occur either via a first-order transition or via two transitions, one of which is a BKT transition and the second is a first-order transition. A detailed description of the situation with computer simulations of melting in two-dimensional systems and an extensive list of publications on this issue can be found in the reviews [17, 19, 20].

2. Berezinskii–Kosterlitz–Thouless transition

As already mentioned above, the BKT transition pertains to three different physical systems that belong to the same universality class and in which similar physical phenomena occur. These are the dissociation of vortex pairs in the X–Y model, charge screening in a 2D Coulomb gas, and the quantum metal–insulator transition in a 1D Luttinger liquid described by the sine-Gordon model [45, 46, 55]. In the first two cases, we are dealing with a classical model of point objects (vortices or charges) interacting via a logarithmic potential, which becomes short-ranged when these objects can move freely and screen the interaction. In the latter case, we are dealing with a quantum 1D model that effectively becomes 2D at $T = 0$. In this case, the dynamic degrees of freedom provide an additional dimension [45, 46].

The BKT transition was originally formulated in the context of the two-dimensional X–Y model, which describes the exchange interaction between classical two-component spins of fixed length $S = 1$.

In the works of Berezinskii, Kosterlitz, and Thouless [13, 15] (see also [16, 17]), it was shown that quasi-long-range order in two-dimensional degenerate systems, to which the X–Y model belongs, is destroyed by the dissociation of bound topological defects. Let us consider this in more detail. The Hamiltonian of the model has the form:

$$H = -\frac{J}{2}\sum_{\langle i\neq j\rangle}\mathbf{S}_i\mathbf{S}_j = -\frac{J}{2}\sum_{\langle i\neq j\rangle}\cos\left(\omega_i-\omega_j\right) \approx \frac{J}{2}\int d^2r\,(\nabla\omega)^2\,, \tag{4}$$

where ω_i is the angle determining the direction of the vector $\mathbf{S}_i$ with respect to an arbitrary axis, i and j are nearest neighbors, and J is the exchange integral.

At low temperatures, the behavior of the system is determined by Gaussian fluctuations. Using the theorem on the mean values of Gaussian-distributed quantities, we find

$$\left\langle \mathbf{S}(\mathbf{r})\mathbf{S}(\mathbf{r}_0)\right\rangle \propto \left\langle \exp\left(\mathrm{i}(\omega(\mathbf{r})-\omega(\mathbf{r_0}))\right)\right\rangle \propto \left(\frac{|\mathbf{r}-\mathbf{r}_0|}{a_0}\right)^{-k_\mathrm{B}T/2\pi J}, \tag{5}$$

where a_0 is the lattice constant. Thus, the system exhibits quasi-long-range order, characterized by a power-law decay of correlations

$$\left\langle \mathbf{S}(\mathbf{r})\mathbf{S}(\mathbf{r}_0)\right\rangle \propto r^{-\eta}\,, \tag{6}$$

while at high temperatures, an exponential decay of correlations occurs

$$\left\langle \mathbf{S}(\mathbf{r})\mathbf{S}(\mathbf{r}_0)\right\rangle \propto \exp\left(-\frac{r}{\xi}\right) \tag{7}$$

(see, e.g., [9]). The mechanism for the destruction of quasi-long-range order was proposed in the aforementioned works of Berezinskii, Kosterlitz, and Thouless. They showed that the destruction of quasi-long-range order occurs through the formation of free topological defects — vortices — which are

described by the equation:

$$\frac{\delta H}{\delta \omega} = J\nabla^2\omega = 0\,, \tag{8}$$

the solution of which has the form:

$$\omega = q\arctan\left(\frac{y}{x}\right); \quad \mathbf{v}_q = \nabla\omega = \frac{q}{r}\,\mathbf{e}_\varphi\,, \tag{9}$$

Here x and y are coordinates in the plane, q is the topological charge of the vortex, with $\oint(\nabla\omega)\,\mathrm{d}l = 2\pi q$, where the integral is taken along a contour around the vortex, $\mathbf{e}_\varphi$ is the unit vector in polar coordinates with origin at the vortex center, and $q = \pm1, \pm2, \ldots$. A vortex is a topological defect that cannot be transformed into the ground state, in which all spins are aligned in the same direction, by means of continuous rotations.

The transition temperature can be determined from simple considerations: the energy of a single vortex is obtained from relations (4) and (9) and has the form:

$$E_v = \frac{J}{2}\int_0^L \frac{2\pi}{r}\,\mathrm{d}r = J\pi\ln\left(\frac{L}{a}\right), \tag{10}$$

where L is the system size. The change in free energy upon the appearance of a vortex is $F = E_v - TS$, where $S = 2k_\mathrm{B}\ln(L/a)$ is the vortex entropy, which is proportional to the logarithm of the system area. The quantity $F = (J\pi - 2k_\mathrm{B}T)\ln(L/a)$ becomes negative at $T \geqslant T_\mathrm{BKT}$, so that the appearance of a vortex becomes energetically favorable, where

$$k_\mathrm{B}T_\mathrm{BKT} = \frac{\pi J}{2}\,. \tag{11}$$

From Eqn (5), it follows that at $T = T_\mathrm{BKT}$, the correlation function has the form: $\langle \mathbf{S}(\mathbf{r})\mathbf{S}(0)\rangle \propto r^{-1/4}$. Thus, at the transition point, the value of the exponent for the correlation function is $\eta = 1/4$.

This simple physical picture, however, is not entirely physically adequate, since bound pairs of oppositely 'charged' vortices do not destroy the quasi-long-range order and have finite energy. Such pairs can exist at low temperatures. The above Hamiltonian for the vortex subsystem is equivalent to the Hamiltonian of a two-component two-dimensional Coulomb gas [15, 55]:

$$H_\mathrm{c} = -\pi J\sum_{i<j} q_i q_j \ln\frac{|\mathbf{r}_i - \mathbf{r}_j|}{a} + E_\mathrm{c}\sum_i q_i^2\,. \tag{12}$$

The harmonic approximation used in deriving (12) is inadequate at small r; therefore, a core energy E_c is introduced to account for the contribution from the region of small r of the order of the core diameter a. E_c plays the role of the chemical potential of the two-dimensional Coulomb gas. For the X–Y model on a square lattice, the chemical potential has the form [77]:

$$E_\mathrm{c} = \frac{\pi^2 J}{2}\,, \tag{13}$$

however, this quantity can, in principle, vary, in particular for the case of superconductors, which leads to significant changes in the nature of the transition. Below, we consider only neutral configurations of the vortex system, in which there are m vortices of one sign ($\sum_i q_i^+ = \sum_i q_i^- = m$). In this case, the partition function corresponding to Hamiltonian (12) can be written as:

$$Z = \sum_{n=1}^{\infty}\frac{1}{(n!)^2}\,y^{2n}\int \mathrm{d}\mathbf{r}_1\ldots\mathrm{d}\mathbf{r}_{2n}\exp\left[\sum_{i<j}^{2n} 2\pi J\ln\left(\frac{r_{ij}}{a}\right)q_i q_j\right], \tag{14}$$

where

$$y = \exp(-\beta E_\mathrm{c})\,. \tag{15}$$

The name 'two-dimensional Coulomb gas' stems from the fact that $V(r) = -1/2\pi\ln(r)$ is the fundamental solution of the Poisson equation in two dimensions:

$$\Delta V(r) = -2\pi\delta(\mathbf{r})\,. \tag{16}$$

The mechanism of the BKT transition [13, 15] is the dissociation of a dilute gas of vortex pairs, and it is necessary to take into account the screening of the Coulomb potential by thermally excited pairs. Dissociation occurs at the temperature at which the dielectric constant of the system diverges. Within the mean-field approximation, the mechanism of vortex–antivortex pair dissociation can be investigated using the Poisson–Boltzmann equation [23, 55, 57], which for the potential $V_\mathrm{s}(r)$ screened by free charges has the form:

$$\Delta V_\mathrm{s}(r) = -2\pi\delta(\mathbf{r}) + \frac{2\pi\rho_\mathrm{F}}{T}\,V_\mathrm{s}(r)\,, \tag{17}$$

where $\rho_\mathrm{F} = \rho_\mathrm{F}^+ + \rho_\mathrm{F}^-$ is the total density of free particles (vortices). The Fourier transform of Eqn (17) can be written as:

$$V_\mathrm{s}(q) = \frac{2\pi}{q^2 + \lambda^{-2}}\,, \tag{18}$$

where

$$\lambda^{-2} = \frac{2\pi\rho_\mathrm{F}}{T}\,. \tag{19}$$

The inverse Fourier transform gives the expression for the screened potential:

$$V_\mathrm{s}(r) \sim \begin{cases} \dfrac{1}{\sqrt{r}}\exp\left(-\dfrac{r}{\lambda}\right), & \lambda \neq \infty, \\ -\ln(r), & \lambda = \infty \end{cases}. \tag{20}$$

Within the picture described by Eqns (19) and (20), it is evident that the screening length λ is related to the presence of free Coulomb charges ρ_F.

The formalism of the two-dimensional Coulomb gas described by the Hamiltonian (12) can be represented in the form of the sine-Gordon theory [45, 46, 55, 77]. Consider the Hamiltonian

$$H_\mathrm{sG} = \frac{1}{2\pi K_\mathrm{sG}}\int \mathrm{d}\mathbf{r}\,(\nabla\varphi)^2 - \frac{g}{\pi}\int \mathrm{d}\mathbf{r}\,\cos(2\varphi)\,. \tag{21}$$

The partition function Z_sG corresponding to the Hamiltonian (21) can be represented as a functional integral over the field φ [78]:

$$Z_\mathrm{sG} = \int D\varphi\exp(-H_0)\sum_{p=0}^{\infty}\frac{1}{p!}\int \mathrm{d}\mathbf{r}_1\ldots\mathrm{d}\mathbf{r}_p\left(\frac{g}{\pi}\right)^p \times\cos\big(2\varphi(\mathbf{r}_1)\big)\ldots\cos\big(2\varphi(\mathbf{r}_\mathrm{p})\big)\,. \tag{22}$$

Here H_0 is the first term in the Hamiltonian (21). Using the relation

$$\cos\left(2\varphi(\mathbf{r}_i)\right) = \frac{\exp\left(2\mathrm{i}\varphi(\mathbf{r}_i)\right) + \exp\left(-2\mathrm{i}\varphi(\mathbf{r}_i)\right)}{2} = \sum_{q=\pm 1} \frac{\exp\left(2\mathrm{i}q\varphi(\mathbf{r}_i)\right)}{2}, \tag{23}$$

and computing the Gaussian integral over H_0 of the exponential from (23), we obtain (see also (5)):

$$\left\langle \exp\left(2\mathrm{i}\sum_i q_i\varphi(\mathbf{r}_i)\right)\right\rangle = \exp\left(2K\sum_{i<j} \ln\left(\frac{r_{ij}}{a}\right) q_i q_j\right). \tag{24}$$

Using Eqns (22) and (24), the partition function of the sine-Gordon system can be written as:

$$Z_{\mathrm{sG}} = \sum_{n=1}^{\infty} \frac{1}{(n!)^2}\left(\frac{g}{2\pi}\right)^{2n} \int \mathrm{d}\mathbf{r}_1 \ldots \mathrm{d}\mathbf{r}_{2n} \times \exp\left(\sum_{i<j}^{2n} 2K_{\mathrm{sG}} \ln\left(\frac{r_{ij}}{a}\right) q_i q_j\right), \tag{25}$$

which coincides with Eqn (14) after the substitution $K_{\mathrm{sG}} = \pi J/k_{\mathrm{B}}T$ and $y = 2\pi\exp(-\beta E_{\mathrm{c}})$.

The BKT theory includes a renormalization-group treatment of screening effects. The theory predicts a continuous transition from the low-temperature phase characterized by quasi-long-range order to the high-temperature disordered phase. In this case, the quantity $K = J/k_{\mathrm{B}}T$ is renormalized at the transition point T_{BKT} to a universal limiting value, which then jumps to zero. The equations describing the renormalization of the system parameters in the vicinity of the transition were obtained in [15]; however, due to a not entirely correct approximation, they could not be solved properly. The inaccuracy was corrected in the work of Young [56], resulting in a system of renormalization-group equations that now has the well-known form [9, 16, 44, 55, 56]:

$$\frac{\mathrm{d}y(l)}{\mathrm{d}l} = \left(2 - \pi K(l,T)\right) y(l), \tag{26}$$

$$\frac{\mathrm{d}K^{-1}(l,T)}{\mathrm{d}l} = 4\pi^3 y^2(l), \tag{27}$$

where $l = \ln(r/a)$ and y is the fugacity [57]. The solution of Eqns (26)–(27) has been discussed repeatedly (see, e.g., [9, 16, 55]), so we will not dwell on it in detail. We only note that these equations are valid for $y \ll 1$. Given that $y \propto \exp(-E_{\mathrm{c}}/k_{\mathrm{B}}T)$, one can conclude that they correspond to the case of a large core energy of the topological defect. This is a very important circumstance, to which we will return below. As a result of solving the system (26), (27), the $y - K^{-1}$ plane is divided into three regions, in the first of which, as $l \to \infty$, the quantity $y \to 0$, while $K^{-1}(l,T)$ tends to a finite renormalized value determined by the initial values $K_0^{-1}(l=0,T)$, which depend on temperature. The transition temperature T_{BKT} is defined as the maximum temperature at which the renormalized value of $K^{-1}(l,T)$ remains finite as $l \to \infty$. At $T = T_{\mathrm{BKT}}$ and $l \to \infty$, we obtain the relation

$$K(l\to\infty, T_{\mathrm{BKT}}) = \frac{J_{\mathrm{r}}(l\to\infty, T_{\mathrm{BKT}})}{k_{\mathrm{B}}T_{\mathrm{BKT}}} = \frac{2}{\pi}, \tag{28}$$

where J_{r} is the renormalized value of the exchange integral.

It should be noted that the expression for the transition temperature obtained using the renormalization-group method formally coincides with the expression for the temperature derived above from simple energy considerations, with the coupling constant replaced by its renormalized value. The physical meaning of the renormalization is quite simple — as $l = \ln(r/a)$ increases, the influence of vortices bound in pairs disappears, and the part corresponding to topological defects disappears from the renormalized Hamiltonian. As a result, quasi-long-range order exists in this region. The remaining two regions of the phase diagram in the $(y - K^{-1})$ plane are characterized by the fact that for any initial values $y_0(l,T)$ and $K_0^{-1}(l,T)$, both quantities diverge as $l \to \infty$.

Above T_{BKT}, the correlation function decays exponentially, with the correlation length diverging exponentially as the transition temperature is approached from above [16, 55, 58]

$$\xi \propto \exp\left(\frac{\mathrm{const}}{|T - T_{\mathrm{BKT}}|^{1/2}}\right). \tag{29}$$

Equations (26), (27) were derived by Kosterlitz [44] (see also the work of Young [56]) within the framework of the two-dimensional Coulomb gas model. Later they were rederived using standard methods of quantum field theory in the works [59–61] using the representation of the partition function of the two-dimensional Coulomb gas through field theory with a Hamiltonian in the sine-Gordon form [55].

In the limit of low vortex density (large core energy of the topological defect), the transition is described within the framework of the renormalization-group method [44] and is a continuous transition of infinite order.

In the works [62, 63], a first-order transition in the two-dimensional Coulomb gas was also found within the framework of sine-Gordon theory.

When fluctuations are taken into account in the system, an exponential divergence of the isochoric heat capacity $C_V(T)$ is observed [58], with the singular part of the heat capacity near the transition point having the form:

$$C_V^{\mathrm{sing}}(T) \propto \xi^{-2}. \tag{30}$$

From Eqns (29) and (30), it can be seen that this divergence corresponds to a very narrow and high peak; therefore, it cannot be detected in either real or computer experiments [58]. A schematic behavior of $C_V(T)$ for the X–Y model is shown in Fig. 9.4.3 in [58]: $C_V(T)$ has an unobservable essential singularity at T_{BKT} and a nonuniversal, model-dependent maximum above T_{BKT}, associated with the entropy released upon dissociation of bound pairs of topological defects (vortices).

An essential feature of the BKT transition is the fact that the derivatives of the free energy of any order coincide on the right and left sides of the transition point [43, 55, 58], i.e., according to the Ehrenfest classification, this is a continuous transition of infinite order. The free energy and its derivatives are continuous at T_{BKT}, but the dependence of the correlation length (29) and other quantities (e.g., the heat capacity (30)) is exponentially singular and cannot be described by a finite number of derivatives, which corresponds to an infinite-order transition.

As already mentioned, the renormalization-group equations are valid for large values of the defect core energy E_{c}. At

the same time, for small values of E_c, the behavior of the system changes qualitatively — the continuous BKT transition transforms into a first-order transition [55, 64–67]. This property of the BKT transition plays a significant role in the description of two-dimensional melting.

In the expansion of the cosine in Eqn (4), we restricted $(\nabla\omega)^2$. At the same time, vortex-free fluctuations should renormalize J due to anharmonicities of the form $(\nabla\omega)^n$. Consider, for example, the anharmonicity of the form $(\nabla\omega)^4$, following the methods described in the book by Patashinskii and Pokrovskii [9]. Let us approximately represent $(\nabla\omega)^4$ as $\langle(\nabla\omega)^2\rangle(\nabla\omega)^2$. In this case, the modified Hamiltonian for the field ω takes the form:

$$H_{\text{eff}} = \frac{J}{2}\left(1 - c\langle(\nabla\omega)^2\rangle\right)\int \mathrm{d}^2 r\,(\nabla\omega)^2\,, \tag{31}$$

where c is some constant. Calculating $\langle(\nabla\omega)^2\rangle$ using the Hamiltonian (4), we obtain:

$$\langle(\nabla\omega)^2\rangle = \frac{T}{J}\int \mathrm{d}^2 k\,\frac{k^2}{k^2} \propto \frac{T}{J}\,. \tag{32}$$

Thus, a correction to the renormalized exchange integral linear in temperature is obtained, $\propto -T/J$. In principle, the next corrections can be calculated in a similar manner; however, as noted in [9], the resulting series will be asymptotic, and the expansion is not applicable near the transition.

To circumvent this difficulty, a variational approach was proposed in [9], based on the consideration of the quadratic Hamiltonian

$$H_0 = \rho_s \frac{J}{2}\int \mathrm{d}^2 r\,(\nabla\omega)^2\,, \tag{33}$$

where ρ_s is the variational parameter. The variational free energy of the system has the form

$$F_{\text{var}} = \langle H\rangle_0 - TS_0\,, \tag{34}$$

where H is the exact Hamiltonian of the system (4), and the averaging is performed over the Gibbs ensemble with the Hamiltonian H_0. S_0 is the entropy of the system with the Hamiltonian H_0. After minimizing F_{var}, an equation for ρ_s is obtained:

$$\rho_s = \exp\left(-\frac{\theta}{\rho_s}\right), \tag{35}$$

where $\theta = T/(4J)$. At $\theta = 0$ $\rho_s = 1$. Equation (35) always has the trivial solution $\rho_s = 0$. At the critical value $\theta_c = \exp(-1)$, a nonzero solution appears discontinuously (see Fig. 29 in [9]). It was found [9] that at the temperature $T = T_{\text{BKT}}$, the contribution of anharmonicities to ρ_s is numerically small.

In the early years after the appearance of the works by Berezinskii [13, 14] and by Kosterlitz and Thouless [15, 43], interest in the theory was not very high. The situation changed after Kosterlitz and Nelson [68] applied the BKT theory to describe the phase transition in a superfluid helium film.

The energy density for a superfluid film has the form [9, 68]:

$$H_{\text{bose}} = \frac{1}{2}\rho_s \int \mathrm{d}^2 r\,\mathbf{v}_s^2(\mathbf{r})\,, \tag{36}$$

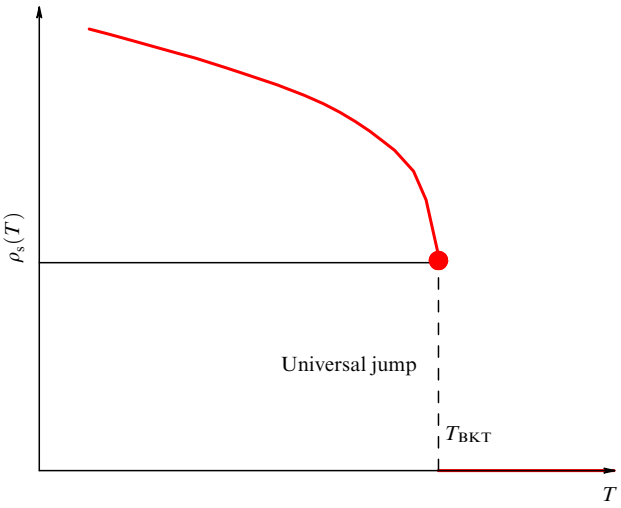

Figure 1. Schematic behavior of the superfluid density $\rho_s = (T)$. The figure illustrates the jump in the superfluid density at $T = T_{\text{BKT}}$ (see Eqn (39)).

where the superfluid velocity $\mathbf{v}_s$ has the form

$$\mathbf{v}_s(\mathbf{r}) = \frac{\hbar}{m}\nabla\omega(\mathbf{r})\,. \tag{37}$$

Thus, the superfluid film is described by a Hamiltonian that coincides in form with (4), with J replaced by $\hbar^2\rho_s(T)/m^2$, where m is the mass of the ^{4}He atom, and $\rho_s(T)$ is the density of the superfluid component. The Hamiltonian of the system in this case can be written as:

$$H_{\text{bose}} = \frac{\rho_s(T)\hbar^2}{2m^2}\int \mathrm{d}^2 r\,(\nabla\omega)^2\,. \tag{38}$$

From Eqn (28), we obtain that for a superfluid helium film, the ratio of the superfluid density to the transition temperature, found theoretically by Kosterlitz and Nelson [68], turned out to be a combination of constants independent of the film thickness:

$$\frac{\rho_s(T_{\text{BKT}})}{k_{\text{B}}T_{\text{BKT}}} = \frac{2m^2}{\pi\hbar^2} = 3.491\times 10^{-9}\ \text{g cm}^{-2}\ \text{K}^{-1}\,. \tag{39}$$

The experiment [47–49, 69] confirmed relation (39) with surprising accuracy, which not only instilled confidence in the correctness of the BKT theory but also stimulated interest in extending the ideas laid down in the works of Berezinskii, Kosterlitz, and Thouless to other systems, primarily to transitions in thin superconducting films and the melting of two-dimensional systems.

It is interesting to note that the BKT phase transition combines features of both discontinuous and continuous transitions: the entropy, area, and even the heat capacity change continuously, but the transverse rigidity (superfluid density) drops discontinuously to zero. A schematic behavior of the superfluid density $\rho_s(T)$ is shown in Fig. 1.

Currently, the experimental study of the BKT transition in Bose–Einstein condensates is primarily focused on the investigation of superfluid states, including vortex behavior, in two-dimensional systems of ultracold atoms in extremely anisotropic quasi-two-dimensional optomagnetic traps (see, e.g., [70–73]).

3. Thin superconducting films

3.1 Canonical Berezinskii–Kosterlitz–Thouless theory

One of the most important manifestations of the BKT transition occurs in quasi-two-dimensional superconducting systems. The experimental successes achieved over recent decades in the study of superconductivity in low-dimensional correlated electron systems have raised new questions about the nature of BKT transitions in real materials, primarily regarding possible limitations of theoretical predictions based on the fundamental ideas of BKT theory, most notably the X–Y model discussed in detail in the previous chapter.

Superconducting films also possess continuous symmetry of the order parameter and are in a certain sense analogous to superfluid films. In them, quasi-long-range order is also destroyed by the dissociation of vortex–antivortex pairs (the BKT transition). It should be noted that in [15], it was erroneously claimed that in a thin superconducting film, the formation of bound vortex–antivortex pairs is impossible because the interaction between vortices at large distances behaves as $1/r$, whereas the BKT transition requires a logarithmic increase of the interaction potential. However, it was later clarified that although in a charged superfluid the logarithmic interaction between vortices is screened by supercurrents [74, 75], for sufficiently thin 'dirty' films with a large bulk penetration depth λ_B, the electromagnetic screening effects are sufficiently weak, so one could expect the occurrence of a BKT transition. The applicability of BKT theory to superconducting films was first discussed in [76]. For an infinite superconducting film of thickness d with bulk penetration depth $\lambda_B(T)$, the vortex interaction energy behaves logarithmically for $r \ll \Lambda(T) = 2\lambda_B(T)/d$ and as $1/r$ for $r \gg \Lambda$ [74, 75]. $\Lambda(T)$ can be regarded as an effective penetration depth for a magnetic field perpendicular to the film plane. It can be expected that a BKT transition may occur if $\Lambda(T)$ exceeds the film size, which can be achieved both by reducing the film thickness and by increasing the degree of disorder in the system, as first noted in [76]. From this, one can conclude that in a superconducting film, a phase transition in the strict sense is absent, since free vortices exist in a superconducting film at all $T > 0$.

In [76], the first attempt was made to construct a phenomenological theory of the BKT transition in thin superconducting films. Using the universal relation between the BKT transition temperature and the superfluid density (39) obtained by Nelson and Kosterlitz, the authors, by analogy, derived an expression relating T_{BKT} to the mean-field Bardeen–Cooper–Schrieffer transition temperature T_{BCS}. The relation between T_{BKT} and T_{BCS} depends on the film resistance [76–78]. To obtain this relation, we start from the well-known Ginzburg–Landau (GL) expansion of the total free energy F in the absence of a magnetic field, which has the form [23, 78, 79]:

$$F = F_n + \int \mathrm{d}^3 r \left[\frac{\hbar^2}{4m} |\nabla \Psi|^2 + a|\Psi|^2 + \frac{b}{2}|\Psi|^2 \right], \tag{40}$$

where the order parameter has the form [80] $\Psi = \sqrt{\rho_s/2}\exp(\mathrm{i}\varphi)$. In the two-dimensional case, the phase fluctuates most strongly, so for thin films we obtain from (40) the Hamiltonian for a thin superconducting film:

$$H_s^{2D} = d \int \mathrm{d}^2 r \frac{\hbar^2}{4m} \frac{\rho_s}{2} (\nabla\varphi)^2 = \frac{\hbar^2 \rho_s^{2D}}{8m} \int \mathrm{d}^2 r (\nabla\varphi)^2 . \tag{41}$$

Here d is the film thickness, $\rho_s^{2D} = \rho_s d$ is the superfluid density in two dimensions. Using the expression for the penetration depth [23, 79, 80]:

$$\lambda^2 = \frac{mc^2}{4\pi e^2 \rho_s} = \frac{mc^2 d}{4\pi e^2 \rho_s^{2D}} , \tag{42}$$

from (42) we obtain

$$\rho_s^{2D} = \frac{\hbar^2 c^2 d}{16\pi e^2 \lambda^2} . \tag{43}$$

Comparing (41) with (4) and using (42) and (43), we obtain the expression for the exchange integral

$$J = \frac{\hbar^2 c^2 d}{16\pi e^2 \lambda^2} . \tag{44}$$

The transition temperature is determined by relation (11)

$$k_B T_{BKT} = \frac{\pi J}{2} = \frac{\varphi_0^2}{16\pi^2} \frac{1}{\Lambda(T_{BKT})} , \tag{45}$$

where $\Lambda = 2\lambda^2/d$ is the effective penetration depth, which significantly exceeds λ, and $\varphi_0 = hc/(2e)$ is the flux quantum. It turned out that in the case of superconductors with impurities, T_{BKT} is below the BCS critical temperature T_{BCS}. At T_{BKT}, the effective penetration depth can be approximately estimated as [76, 78]:

$$\Lambda(T_{BKT}) = \frac{\varphi_0^2}{16\pi^2} \frac{1}{T_{BKT}} \approx \frac{1}{T_{BKT}} \,\mathrm{cm} . \tag{46}$$

Then, using the dirty-limit expression [81] for the penetration depth for very thin films, an estimate of Λ and T_{BKT} in terms of the material parameters of the system was obtained in [76]:

$$\Lambda = \frac{\lambda_L^2(0)}{2d} \frac{\xi_0}{l} \left\{ \frac{\Delta(T)}{\Delta(0)} \tanh\left[\frac{\beta\Delta(T)}{2} \right] \right\}^{-1} . \tag{47}$$

Here λ_L is the London penetration depth, Δ is the energy gap, ξ_0 is the BCS coherence length, and l is the mean free path. This expression can be rewritten as:

$$\Lambda = 1.78 \frac{\varphi_0^2}{8\pi^5} \frac{e^2}{\hbar} \frac{R}{k_B T_{BCS}} f^{-1}\left(\frac{T}{T_{BCS}} \right) . \tag{48}$$

$R = \rho/d$ is the sheet resistance of the film, T_{BCS} is the mean-field BCS transition temperature of the film, and $f(T/T_{BCS})$ is the expression in braces in (47). Substituting Eqn (48) into Eqn (46), one can arrive at an implicit relation between T_{BKT} and T_{BCS}, which depends on fundamental constants and the sheet resistance and has the form:

$$\frac{T_{BKT}}{T_{BCS}} f^{-1}\left(\frac{T}{T_{BCS}} \right) = 0.561 \frac{\pi^3}{8} \left(\frac{\hbar}{e^2} \right) \frac{1}{R} \approx 2.18 \frac{R_c}{R} , \tag{49}$$

where $R_c = \hbar/e^2$ corresponds to a sheet resistance equal to 4.12 kΩ/S. Near the transition temperature, Eqn (49) takes the form:

$$\frac{T_{BKT}}{T_{BCS}} = \left[1 + 0.173 \frac{R}{R_c} \right]^{-1} . \tag{50}$$

From (50), it follows that a substantial suppression of $T_{\rm BKT}$ below $T_{\rm BCS}$ requires a high sheet resistance. In thin, high-resistance films, as the temperature decreases, the BCS (mean-field) transition temperature is reached first, with the BKT transition temperature being attained at a lower temperature. This scenario, involving two characteristic temperatures, is a common feature of the application of these ideas to physical systems. The complete solution of Eqn (49) based on literature data is presented in Fig. 1 of [76]. Since free vortices will be driven by displacement currents through the sample and thus cause dissipation, thin-film superconductors exhibit finite resistance for $T_{\rm BKT} < T < T_{\rm BCS}$. Although the $R(T)$ curves are smooth and continuous at $T_{\rm BCS}$, this is the temperature at which the superconducting gap actually closes, i.e., the order parameter exists above $T_{\rm BKT}$ up to $T_{\rm BCS}$, and this $T_{\rm BCS}$ must be consistent with the $T_{\rm BKT}$ determined from the analysis of fluctuation conductivity. Within the framework of BKT theory, one should expect, as suggested by Halperin and Nelson in [82], that as T decreases, a GL fluctuation regime is first observed, followed by a BKT fluctuation regime between the mean-field temperature $T_{\rm BCS}$ (which could be observed in the three-dimensional case) and the temperature $T_{\rm BKT}$. Halperin and Nelson considered the transition in superconducting films by combining the GL phenomenological picture with an analog of the theoretically predicted jump in superfluid density in neutral superfluids, which allowed them to obtain a useful expression for the resistance [82]:

$$\frac{R}{R_n} = 10.8b \exp\left(-2\sqrt{\frac{b\tau_{\rm c}}{\tau}}\right), \tag{51}$$

where $\tau = (T - T_{\rm BKT})/T_{\rm BKT}$, $\tau_{\rm c} = (T_{\rm BCS} - T_{\rm BKT})/T_{\rm BKT}$ and $\tau \ll \tau_{\rm c}$ and b is a dimensionless fitting parameter of order unity. In this temperature range, the resistance is due to the motion of unbound vortices driven by applied currents. Within BKT theory, the superconducting fluctuation correlation length $\xi \propto \exp\left(\text{const}/|T - T_{\rm BKT}|^{1/2}\right)$ decays exponentially (29) [16, 55], in contrast to the dependence $\xi_{\rm GL}^2 \propto 1/(T - T_{\rm c})$ expected in GL theory [79, 80]. Consequently, by direct measurement of paraconductivity or diamagnetism near the transition, it became possible to detect the onset of vortex fluctuations, which lead to the exponential temperature dependence of the superconducting correlation length.

The dependence of the temperature $T_{\rm BKT}$ on the thickness of superconducting films and the behavior of the difference between the BKT and BCS temperatures have been experimentally studied in a number of works. In [83], crystalline atomically flat Pb films containing an integer number of atomic layers grown on Si(111) by molecular beam epitaxy were investigated, which made it possible to systematically study the nature of superconductivity in two-dimensional films using a combination of scanning tunneling microscopy/spectroscopy (STM/STS) and transport measurements. It turned out that the observed features in sufficiently thin films are consistent with BKT physics. In particular, BCS pairing and superconductivity disappear at two different temperatures, the current-voltage characteristics in the intermediate phase are nonOhmic, and the temperature and current dependences of the resistance agree with the expectations of BKT theory. The authors also showed that Eqn (51) well describes the behavior of R/R_n and yields reasonable transition temperatures for films with d less than 16 atomic layers. For thicker films, R/R_n drops sharply at the superconducting transition temperature, resembling the behavior for a bulk superconductor. For films with $d \leqslant 9$ atomic layers, the value of $T_{\rm BKT}$ derived using Eqn (51) saturates sharply at 6.6 ± 0.15 K, which is identical to $T_{\rm BCS}$ of the films, indicating that these films are in the 3D limit and the transition is of BCS nature. The dependence of the superconducting density on film thickness was also considered in [84, 85].

In [86], the BKT transition in superconducting NbN nanofilms with thickness less than 15 nm on different substrates was considered for different film thicknesses. For this purpose, the universal jump of the superconducting electron density predicted by BKT theory at the temperature $T_{\rm BKT}$ was examined. This jump is associated with the formation of bound vortex–antivortex pairs through the logarithmic interaction potential between free vortices. A current passing through the sample can break bound pairs, creating free vortices that cause nonlinear effects in the I–V curves. The idea is that the current acts on a vortex with a Magnus force (analogous to the hydrodynamic force that occurs when a sphere is immersed in a flow) in the direction perpendicular to the current. This force is opposite for vortices and antivortices and thus can break vortex–antivortex pairs. Free vortices lead to dissipation and the appearance of resistance. This results in a nonlinear current-voltage characteristic [77, 78]:

$$V \propto I^{a(T)}, \quad a(T) = \frac{\pi J_{\rm s}(T)}{T} + 1\,. \tag{52}$$

From Eqn (28), it follows that a should change discontinuously from $a = 3$ at $T_{\rm BKT}^-$ to $a = 1$ at $T_{\rm BKT}^+$. Below $T_{\rm BKT}$, an increase in the exponent a is expected with decreasing T, since the superfluid density increases. The detection of the superfluid density jump from the exponent a was one of the first manifestations of BKT physics in thin superconducting films [87, 88]. Later, it was used to describe the BKT transition in several systems [86, 89], even when its application may be questionable (see, e.g., [89] and the discussion therein). The main problem is determining the correct temperature and current range where Eqn (52) can be applied. Nonlinearity is expected only below $T_{\rm BKT}$. In real samples, even below $T_{\rm BKT}$, finite-size effects always lead to a finite number of free vortices ρ_v even for $I \to 0$, which is orders of magnitude smaller than the value of this quantity in the normal state [90]. Thus, the effect of the appearance of free vortices will manifest in experiments as a deviation from linear (Ohmic) behavior of the current-voltage characteristic to nonlinear behavior when I exceeds a threshold value I^* for the dissociation of vortex–antivortex pairs [86, 89, 91]. This also means that one should avoid confusion between the threshold current for breaking vortex pairs and the actual critical current of the superconductor, at which Cooper pairs are destroyed. In [89], it was shown how, taking into account the effect of inhomogeneity on the smearing of the superfluid density jump, one can obtain agreement between the dependence $J_{\rm s}(T)$ obtained from direct measurements of the inverse penetration depth via mutual inductance of two coils in NbN and the dependence obtained from the exponent of the I–V characteristic (52).

As discussed above, to observe the BKT transition in thin superconducting films, it is first necessary that the sample width be smaller than Λ. In addition, the external field must be sufficiently small. This is because the resistance in a field

$H > H_{c1}$ is proportional to the total number of free vortices, including contributions from both field-induced vortices and unbound pairs [92]. Moreover, since in a field it is energetically more favorable to have vortices than antivortices, the external field can induce pair dissociation below T_{BKT}. Consequently, to ensure that the measured value of R/R_n corresponds to the BKT transition, i.e., is determined by the dissociation of vortex–antivortex pairs above T_{BKT}, measurements must be performed in sufficiently weak external fields. In this regard, we note a recent work [93] in which the BKT transition in ultrathin NbN films is investigated in the presence of weak perpendicular magnetic fields. The jump in the phase stiffness at the BKT transition is observed up to 5 G, while the BKT features are smeared between 5 G and 50 G, disappearing completely at 100 G, where ordinary current–voltage behavior corresponding to a BCS-type transition is observed. The obtained results show that weak magnetic fields, negligible in bulk systems, significantly affect the ultrathin film, promoting a transition from Halperin–Nelson fluctuations to a BCS-like state with Ginzburg–Landau fluctuations as the field increases. This behavior is associated with field-induced free vortices, which screen the vortex–antivortex interaction and smear the BKT transition.

It is also necessary that vortex pinning be sufficiently weak. Although all developed theoretical models have not yet consistently considered the effect of random pinning on the transition in thin superconducting films, pinning is inevitable, especially when using a 'dirty' superconductor with high resistance. If a vortex in a bound pair is pinned, under the influence of displacement currents it may be more favorable for it not to move and to break the pair rather than remain as an intact pair. Therefore, in the presence of pinning, additional dissociation of vortex–antivortex pairs and trapping of free vortices can alter the temperature dependence of the resistance and broaden the transition. All these factors complicate the analysis of experimental results.

Thus, the case of thin superconducting films represents one of the most extensively studied examples of the application of BKT physics. In principle, in this case there are several opportunities for experimental investigation of specific manifestations of BKT physics. For example, upon approaching the transition at $T < T_{BKT}$, by analogy with a thin superfluid film, the superfluid density ρ_s is expected to tend to zero as the BKT temperature T_{BKT} is approached (see Fig. 1), with a universal relation between $\rho_s(T_{BKT})$ and the temperature T_{BKT} itself (39). When approaching the transition from above, in principle, there is a possibility to identify the BKT transition through the temperature dependence of superconducting fluctuations.

Interestingly, measurements of the universal BKT jump of the superfluid density have become available only relatively recently [84, 85, 94–97], due to improvements in experimental methods driven mainly by research on high-temperature superconductors in the late 1990s. In particular, the use of the two-coil mutual inductance technique [98] proved crucial for obtaining the absolute value of the superfluid density at zero temperature, which is necessary for comparing experimental data with BKT predictions. Studies employing terahertz spectroscopy [99–101] have proven very productive, as they allow measurement of the analog of the superfluid density jump at a finite frequency.

From the above brief review of the available experimental and theoretical results, one can conclude that BKT physics has been clearly observed in some cases, but often in the literature the observation of BKT manifestations has been based on a naive application of the famous canonical BKT formulas. This must be taken into account in order to adopt a sufficiently critical attitude toward manifestations of the BKT transition in experiment. This primarily concerns the problem of broadening of the observed transition, which has been attempted to be explained semi-phenomenologically by invoking paraconductivity, disorder effects, etc. At the same time, to a large extent the problem lies in the fact that a truncated form of the vortex-vortex interaction is considered, taking into account only the logarithmic part. A calculation variant based on the full potential is presented in the following paragraph.

3.2 Berezinskii–Kosterlitz–Thouless-type transition in a thin superconducting film (the ring approximation)

The specific nature of the vortex interaction in a thin superconducting film does not allow the dissociation of vortex–antivortex pairs (the BKT transition) to be described by following a straightforward analogy with the X–Y model or the vortex system in a thin superfluid film.

In this section, we consider an approach to describing this transition based on the use of the ring approximation for calculating the thermodynamic quantities of a vortex system with long-range vortex–vortex interaction obtained in the famous work of Pearl [74]. It should be noted that sometimes a misunderstanding arises regarding the nature of the vortices in a thin superconducting film that cause the BKT-type transition. These vortices are of the same nature as Abrikosov vortices in a bulk superconductor and transform into them as the film thickness increases. The form of correction terms to the Pearl solution taking into account the film thickness was obtained in [75].

Due to the fact that the vortex–vortex interaction at large distances has the form $\Phi \propto 1/r$, at $T > 0$ a superconducting film always has a finite density of free vortices, $\varrho_{\pm}$, with magnetic moment parallel $(+)$ or antiparallel $(-)$ to the external magnetic field H, respectively. These free vortices are responsible for energy dissipation and cause a resistance 'tail' in the low-temperature region. The resistance is given by the Bardeen–Stephen formula [81]

$$\frac{R}{R_N} = 2\pi\xi^2(\varrho_+ + \varrho_-)\,, \tag{53}$$

where R is the resistance caused by vortex motion and R_N is the resistance of the film in the normal state, and ξ is the correlation length. Consequently, in order to calculate the resistance of a superconductor due to vortex motion, it is necessary to obtain relations for the density of free vortices as a function of temperature and field.

As discussed in Section 3, the existence of a Kosterlitz–Thouless-type transition is confirmed experimentally [55, 84, 85, 87, 88, 94, 99, 100, 102–106].

At the same time, there are obvious shortcomings in the theoretical description of the behavior of a superconducting film using the two-dimensional Coulomb gas model. The form of the function R/R_N obtained using the renormalization-group equations can be justified only in a narrow temperature interval $T_{BKT} < T \ll T_{BCS}$, while the majority of experimental results pertain to temperatures outside this region. In the temperature range sufficiently close to T_{BKT}, the renormalization-group method is not applicable to superconductors [55]. Moreover, the resistance 'tail' in the low-temperature region cannot be described within the frame-

work of BKT theory, but requires additional semi-phenomenological approaches (paraconductivity, pinning).

In this section, we discuss a statistical theory of a vortex plasma in two-dimensional superconductors, which overcomes some of the difficulties mentioned above and offers a way to calculate the quantities on the right-hand side of Eqn (53) in the entire temperature range $0 < T < T_c$. The presentation is based on the works [107–111].

Ring approximation for the vortex system in a two-dimensional superconductor. Consider the free energy of a system of N vortices ($N = N_+ + N_-$), whose coordinates in a sample of thickness d have the form $\mathbf{r}_i(z) = (x_i(z), y_i(z))$, $i = 1, \ldots, N$ (the external field H is directed along the z-axis). Let ε be the energy per unit length of a vortex and $\varphi_0 = hc/2e$ be the flux quantum.

The interaction energy of two vortices located at points $\mathbf{r}_i$ and $\mathbf{r}_j$ ($r_{ij} = |\mathbf{r}_i - \mathbf{r}_j| \gg \xi$) has the form [74]

$$\Phi(r_{ij}) = \frac{\varphi_0^2}{8\pi\Lambda}\left[H_0\left(\frac{r_{ij}}{\Lambda}\right) - Y_0\left(\frac{r_{ij}}{\Lambda}\right)\right],$$
$$\Phi(r_{ij}) \approx -\frac{\varphi_0^2}{4\pi^2\Lambda}\ln\left(\frac{r_{ij}}{\Lambda}\right) \quad r_{ij} \ll \Lambda,$$
$$\Phi(r_{ij}) \approx \frac{\varphi_0^2}{4\pi^2 r_{ij}} \quad r_{ij} \gg \Lambda. \tag{54}$$

Here H_0 is the Struve function and Y_0 is the Neumann function. Corrections to this energy due to the small but finite film thickness were obtained in [75].

For a thin superconducting film, the energy per unit length of a vortex ε has the form [74]

$$\varepsilon = \pi r_0^2 \xi^2\left(\frac{H_c^2}{8\pi}\right) + \frac{\varphi_0^2}{16\pi\Lambda d}\left(H_0\left(\frac{\xi}{\Lambda}\right) - Y_0\left(\frac{\xi}{\Lambda}\right)\right), \tag{55}$$

where the first term represents the contribution from the vortex core, r_0 is the vortex core radius (in units of ξ), and H_c is the thermodynamic critical field.

The canonical partition function for the system described by Eqn (54) has the form [107–111]:

$$Z_N = \frac{z_+^{N_+} z_-^{N_-}}{N_+! N_-!}\int \mathrm{d}\mathbf{r}_1 \ldots \int \mathrm{d}\mathbf{r}_N \exp\left\{-\frac{\beta}{2}\sum_{i\neq j} s_i s_j \Phi(r_{ij})\right\}, \tag{56}$$

where $\beta = 1/k_B T$, the activities z_+ and z_- have the form $z_\pm = \Gamma \exp(\beta\mu_\pm)$ and $\mu_+ = -(\varepsilon - \varphi_0 H/4\pi)d$; $\mu_- = -(\varepsilon + \varphi_0 H/4\pi)d$.

Let us estimate the constant Γ. Setting $N = 1$ and $H = 0$ in Eqn (56), we obtain ($z_+ = z_- = z$)

$$Z_1 = z\Omega. \tag{57}$$

The free energy of a vortex corresponding to the partition function Z_1 should be equal to the formation energy of a single vortex oriented perpendicular to the film (assuming the limit $L \to \infty$)

$$F_{vor} = \varepsilon d - TS. \tag{58}$$

The entropy S has the form $S = \ln(\Omega/\zeta)$, where ζ is the area occupied by a vortex and Ω is the film area. It is assumed that ζ is proportional to the region occupied by the vortex core, $\zeta = c\xi^2$, where c is a temperature-independent constant [55]. Using (57) and (58), we obtain:

$$\Gamma = \frac{1}{c\xi^2}. \tag{59}$$

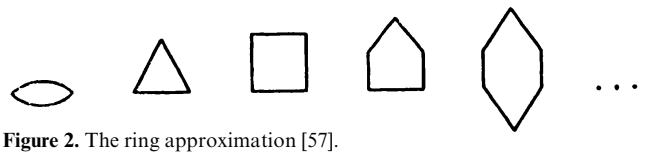

Figure 2. The ring approximation [57].

In this case, the grand partition function has the form

$$Z = \sum_{N_+, N_- = 0} \frac{z_+^{N_+} z_-^{N_-}}{N_+! N_-!}\int \mathrm{d}\mathbf{r}_1 \ldots \int \mathrm{d}\mathbf{r}_N \exp\left\{-\frac{\beta}{2}\sum_{i\neq j} s_i s_j \Phi(r_{ij})\right\}. \tag{60}$$

The sum is taken over all configurations with different N_+ and N_-.

The Gibbs free energy associated with (60) is equal to [112]

$$G = -k_B T \ln Z = k_B T\left\{\varrho_+\left[\ln\left(\frac{\varrho_+}{z_+}\right) - 1\right] + \varrho_-\left[\ln\left(\frac{\varrho_-}{z_-}\right) - 1\right] - S\right\}\Omega, \tag{61}$$

$$S = \sum_{n_+ + n_- \geqslant 2}\sum_{n_+}\sum_{n_-} \beta_{n_+ n_-}\varrho_+^{n_+}\varrho_-^{n_-}, \tag{62}$$

where $\beta_{n_+ n_-}$ is the sum of irreducible Mayer diagrams [112] ($v = n_+ + n_-$),

$$\beta_{n_+ n_-} = [n_+! n_-! \Omega]^{-1}\int \mathrm{d}\mathbf{r}_1 \ldots \mathrm{d}\mathbf{r}_v \sum\prod f_{ij},$$
$$f_{ij} = \exp\left[-\beta\Phi(r_{ij})\right] - 1. \tag{63}$$

The induction B is related to the densities of free vortices ϱ_+ and ϱ_- by the relation $B = \varphi_0(\varrho_+ - \varrho_-)$. Substituting this expression into (61) gives G as a function of T, H, ϱ_+ and ϱ_-.

To obtain equations for ϱ_+ and ϱ_-, one can use the virial expansion [57, 112]

$$\varrho_\pm = z_\pm \exp\left\{\frac{\partial}{\partial\varrho_\pm} S\right\}. \tag{64}$$

Note that Eqn (64) can be obtained from the extremum condition of the free energy G:

$$\frac{\partial G}{\partial\varrho_+} = \frac{\partial G}{\partial\varrho_-} = 0. \tag{65}$$

Due to the long-range nature of the interaction (54), a problem arises with the convergence of individual terms in the Mayer expansion (62). This problem can be solved using the ring approximation, well known from plasma physics (2).

In this approximation, we have [57]

$$S = \sum_{v \geqslant 2} S_v$$
$$S_v = \sum_{n_+}\sum_{n_-} \frac{(v-1)!}{2}\frac{(-\beta\varrho_+)^{n_+}}{n_+!}\frac{(-\beta\varrho_-)^{n_-}}{n_-!} J_v$$
$$= \frac{1}{2v}\left[-\beta(\varrho_+ + \varrho_-)\right]^v J_v, \tag{66}$$

where $J_v = \Omega^{-1}\int \mathrm{d}\mathbf{r}_1 \ldots \mathrm{d}\mathbf{r}_v\, \Phi(r_{12})\Phi(r_{23})\ldots\Phi(r_{v1})$. J_v can be calculated using the Fourier transform, taking into account that the Fourier transform $\tilde{\Phi}(q)$ of the potential (54) has the

form:

$$\tilde{\Phi}(q) = \frac{\varphi_0^2}{2\pi\Lambda} \frac{1}{q(q+1/\Lambda)} \,. \tag{67}$$

The possibility of calculating the sum of ring diagrams is based on the special form of the quantity (67). It is easy to see that for the standard Coulomb potential $\Phi_c \propto 1/r$, whose Fourier transform has the form $\propto 1/k^2$, the sums of ring diagrams diverge. Calculations using Eqns (66) and (67) show that

$$-4\pi S = \begin{cases} \dfrac{1}{2}\kappa^2 - \dfrac{1}{2}\left(\kappa^2 - \dfrac{1}{2\Lambda^2}\right)\ln(\kappa^2\Lambda^2) - \dfrac{\omega}{\Lambda}\arctan(2\omega\Lambda), \\ \qquad\qquad \kappa^2 - \dfrac{1}{4\Lambda^2} \geqslant 0, \\ \dfrac{1}{2}\kappa^2 - \dfrac{1}{2}\left(\kappa^2 - \dfrac{1}{2\Lambda^2}\right)\ln(\kappa^2\Lambda^2) + \dfrac{\sigma}{2\Lambda}\ln\dfrac{1+2\Lambda\sigma}{1-2\Lambda\sigma}, \\ \qquad\qquad \kappa^2 - \dfrac{1}{4\Lambda^2} < 0, \end{cases} \tag{68}$$

where $\kappa^2 = \beta(\varrho_+ + \varrho_-)\varphi_0^2/2\pi\Lambda, \omega = \sqrt{\kappa^2 - 1/4\Lambda^2}, \sigma = \sqrt{1/4\Lambda^2 - \kappa^2}$

Vortex system in the absence of a magnetic field. Let us discuss the properties of a superconducting magnetic film in the absence of an external magnetic field. In this case, $\varrho_+ = \varrho_- = 1/2\,\varrho$, $z_+ = z_- = z$. Substituting (68) into (64) gives

$$\varrho = 2z\exp\left\{\beta\frac{\varphi_0^2}{16\pi^2\Lambda}\left(\ln(\kappa^2\Lambda^2) + \frac{1}{\omega\Lambda}\arctan(2\omega\Lambda)\right)\right\}, \quad \kappa^2 - \frac{1}{4\Lambda^2} \geqslant 0, \tag{69}$$

$$\varrho = 2z\exp\left\{\beta\frac{\varphi_0^2}{16\pi^2\Lambda}\left(\ln(\kappa^2\Lambda^2) + \frac{1}{2\sigma\Lambda}\ln\frac{1+2\sigma\Lambda}{1-2\sigma\Lambda}\right)\right\}, \quad \kappa^2 - \frac{1}{4\Lambda^2} < 0, \tag{70}$$

where $\kappa^2 = \beta\varrho\varphi_0^2/2\pi\Lambda$.

Using Eqns (61) and (68), one can write $G(T)$ in the form

$$\frac{G(T)}{k_B T\Omega} = \varrho\left[\ln\left(\frac{\varrho}{2z}\right) - 1\right] + \frac{1}{4\pi} \times \begin{cases} \dfrac{1}{2}\kappa^2 - \dfrac{1}{2}\left(\kappa^2 - \dfrac{1}{2\Lambda^2}\right)\ln(\kappa^2\Lambda^2) - \dfrac{\omega}{\Lambda}\arctan(2\omega\Lambda), \\ \qquad\qquad \kappa^2 - \dfrac{1}{4\Lambda^2} \geqslant 0, \\ \dfrac{1}{2}\kappa^2 - \dfrac{1}{2}\left(\kappa^2 - \dfrac{1}{2\Lambda^2}\right)\ln(\kappa^2\Lambda^2) + \dfrac{\sigma}{2\Lambda}\ln\dfrac{1+2\Lambda\sigma}{1-2\Lambda\sigma}, \\ \qquad\qquad \kappa^2 - \dfrac{1}{4\Lambda^2} < 0. \end{cases} \tag{71}$$

Substituting Eqns (69) and (70) into (72), one can write the free energy in the form of an 'equation of state' [57, 107–112]

$$\frac{P}{k_B T} = \varrho - 2\varrho\frac{\partial S}{\partial\varrho} + S,$$

where the pressure in the vortex plasma has the form $P = -G(T)/\Omega$.

The behavior of ϱ for T near T_{BKT} and for small T can be obtained in explicit form. Let us consider these cases.

As $T \to 0$, as can be seen from Eqn (70), the vortex density $\varrho \to 0$

$$\varrho = \frac{2}{c\xi^2}\exp\left(-\frac{\varepsilon d}{k_B T}\right). \tag{72}$$

Now let us consider approximate solutions of Eqns (69) and (70) near T_{BKT}. In this case, it is necessary to solve Eqn (69), since the inequality $\kappa^2 - 1/4\Lambda^2 \geqslant 0$ holds for nonzero ϱ and sufficiently small thickness d. In the limit of small d, the second term in the exponent of (69) can be neglected, and Eqn (69) reduces to

$$\kappa^2\Lambda^2 = \frac{z\beta\varphi_0^2\Lambda}{\pi}\exp\left\{\beta\frac{\varphi_0^2}{16\pi^2\Lambda}\ln(\kappa^2\Lambda^2)\right\}. \tag{73}$$

The solution of Eqn (73) has the form

$$\varrho = \frac{2\pi k_B T}{\varphi_0^2\Lambda}\, q^{k_B T/(k_B T - \Theta(T))}, \tag{74}$$

where $q = z\beta\varphi_0^2\Lambda/\pi$ and $\Theta(T) = \varphi_0^2/(16\pi^2\Lambda(T))$. Equation (74) is similar to the equation used to describe the Kosterlitz–Thouless transition [55]. According to Eqn (74), $\varrho \to 0$ as $T \to T_{BKT}$ from above, where T_{BKT} is determined by the equation $k_B T_{KT} = \Theta(T_{BKT})$ (see Eqn (45)) (provided that $q < 1$). It should be noted that for the exact Eqns (69) and (70), there is no phase transition in the sense that the vortex density ϱ never vanishes exactly; however, ϱ changes very rapidly near T_{BKT} due to the dissociation of vortex–antivortex pairs.

The parameters for specific calculations are taken from the experimental work [106], in which the properties of a Nb film with thickness 20 Å were studied in detail. In this case,

$$\xi(t) = \frac{\xi(0)}{\sqrt{1-t}}\,, \quad \lambda_B(t) = \frac{\lambda(0)}{\sqrt{1-t}}\,, \tag{75}$$

where $t = T/T_{BCS}$, $T_{BCS} \simeq 3.66$ K, $\xi(0) \simeq 104$ Å, and $\lambda(0) \simeq 1600$ Å. T_c is defined as the temperature at which $R = 0.5R_N$. From this condition, the constant c can be determined. Using (53), (59), and (69), we obtain $c = 6\pi$. The behavior of the system depends on the choice of the core radius r_0. In general, r_0 can be considered as a fitting parameter.

Dependence of the phase transition on the vortex core radius (or on the vortex core energy). As discussed above, there exists a dependence of the form of the solutions of Eqns (69) and (70) on the vortex core radius r_0 due to the connection between r_0 and the vortex core energy (55).

Let us rewrite Eqn (69) in the form (see Eqn (74))

$$\varrho = \frac{2\pi k_B T}{\varphi_0^2\Lambda}\, q^{k_B T/(k_B T - \Theta(T))} \times \exp\left\{\frac{\Theta(T)}{k_B T - \Theta(T)}\frac{1}{\omega\Lambda}\arctan(2\omega\Lambda)\right\}. \tag{76}$$

From Eqn (76), it can be seen that for $q < 1$, the density of free vortices $\varrho \to \infty$ as T approaches T_{BKT} from below. On the other hand, for $q > 1$, the density ϱ diverges as T_{BKT} is approached from above. The critical value of the vortex core radius r_0^c can be obtained from the equation $q(T_{BKT}, r_0) = 1$ and is equal to 1.2237.

The behavior of the solutions of Eqns (69) and (70) (see [107–109]) can be regarded as an indication that for $r_0 < r_0^c$,

the dissociation of vortex pairs occurs via a first-order transition. However, it should be noted that there are obvious shortcomings in these solutions. First of all, the density of free vortices diverges as $T_{\rm BKT}$ is approached from above. Moreover, there is a narrow region near $T_{\rm BKT}$ where the solution is not defined. A possible reason for the divergence of the free vortex density may be the assumption of point-like vortices, which was used in deriving Eqns (69), (70), and (72), with the core radius entering the equations only through the vortex core energy.

To take into account the finite size of the vortex core, we write the interaction energy in the form [55]:

$$\tilde{\Phi}(r) = \int \mathrm{d}^2 r' \, \mathrm{d}^2 r'' \, n\left(|\mathbf{r} - \mathbf{r}'|\right) \Phi\left(|\mathbf{r}' - \mathbf{r}''|\right) n\left(r''\right), \qquad (77)$$

where $n(r)$ denotes the charge distribution of a single vortex, $\int n(r)\ \mathrm{d}^2 r = 1$.

The Fourier transform of the potential $\tilde{\Phi}(r)$ has the form:

$$\tilde{\Phi}_q = \frac{\varphi_0^2}{2\pi\Lambda} \frac{n_q^2}{q(q + 1/\Lambda)}, \qquad (78)$$

where

$$n_q = \int \mathrm{d}^2 r \, \exp\left(\mathrm{i}\mathbf{q}\mathbf{r}\right) n\left(r\right) \qquad (79)$$

is the Fourier transform of the charge distribution of a single vortex $n(r)$. $n(r)$ vanishes as $r \to \infty$ and $n(r) \neq 0$ in the vicinity of $r \leqslant \xi$.

Using the ring approximation, one can readily show that the free energy G for nonpoint-like vortices with interaction (77) has the form:

$$\frac{G}{k_{\rm B} T \Omega} = 2\rho \left[\ln\left(\frac{\rho}{2z}\right) - 1 \right] + \frac{1}{8\pi^2} \int \mathrm{d}^2 q \left\{ \ln\left(1 + \kappa^2 \tilde{u}_q\right) - \kappa^2 \tilde{u}_q \right\}, \qquad (80)$$

where

$$\tilde{u}_q = \frac{n_q^2}{q(q + 1/\Lambda)}. \qquad (81)$$

To obtain the equation for ρ, one can use the virial expansion [112] or the extremum condition for the energy G:

$$\frac{\partial G}{\partial \rho} = 0. \qquad (82)$$

From Eqns (80) and (82), we have:

$$\ln\left(\frac{\rho}{2z}\right) = -\frac{1}{8\pi^2} \frac{\partial}{\partial \rho} \int \mathrm{d}^2 q \left\{ \ln\left(1 + \kappa^2 \tilde{u}_q\right) - \kappa^2 \tilde{u}_q \right\}. \qquad (83)$$

Let us choose the distribution $n(r)$ in the form:

$$n(r) = \int_{q \leqslant B} \frac{\mathrm{d}^2 q}{4\pi^2} \exp\left(-\mathrm{i}\mathbf{q}\mathbf{r}\right). \qquad (84)$$

From this equation, we obtain:

$$n_q = \begin{cases} 1, & q \leqslant B \\ 0, & q > B \end{cases}. \qquad (85)$$

Note that the behavior of the two-dimensional Coulomb gas depends little on the detailed form of the charge distribution [62, 63]. Similarly, one can assume that the simple equations (84) and (85) are sufficient to describe the dissociation of vortex–antivortex pairs in a two-dimensional superconductor. In order to determine the parameter B, note that two vortices of opposite signs placed at the same point must annihilate. The energy of two opposite vortices perpendicular to the plane of the superconductor and located at a distance r from each other can be written as

$$\Delta F_{\rm pair}(r) = 2\varepsilon + \tilde{\Phi}(r), \qquad (86)$$

where the energy of a single vortex is given by (see Eqn (55)):

$$\varepsilon = \pi r_0^2 \xi^2 d \left(\frac{H_{\rm c}^2}{8\pi} \right) + \frac{\varphi_0^2}{16\pi\Lambda} \left(H_0\left(\frac{\xi}{\Lambda}\right) - Y_0\left(\frac{\xi}{\Lambda}\right) \right). \qquad (87)$$

Using the condition $\Delta F_{\rm pair}(0) = 0$, we obtain an equation for B. It can be shown that $B \simeq 1/\xi$ in the case $\xi \ll \Lambda$, i.e., in the limit $\xi \to 0$, we have $n(r) \to \delta(r)$.

Using Eqns (85) and (83), we obtain

$$\ln\left(\frac{\rho}{2z}\right) = \frac{\beta\varphi_0^2}{16\pi^2\Lambda} \left\{ \ln\left(\frac{(B+1)^2}{B^2 + B + \zeta} \zeta \right) + J(B, \zeta) \right\}, \qquad (88)$$

where

$$J(B,\zeta) = \frac{2}{\sqrt{4\zeta - 1}} \left\{ \arctan\frac{2B+1}{\sqrt{4\zeta - 1}} - \arctan\frac{1}{\sqrt{4\zeta - 1}} \right\}, \ 4\zeta - 1 \geqslant 0,$$

$$J(B,\zeta) = \frac{1}{\sqrt{4\zeta - 1}} \ln\left(\frac{2B + 1 - \sqrt{1 - 4\zeta}}{2B + 1 + \sqrt{1 - 4\zeta}} \right) \left(\frac{1 + \sqrt{1 - 4\zeta}}{1 - \sqrt{1 - 4\zeta}} \right), \ 4\zeta - 1 \leqslant 0, \qquad (89)$$

and $\zeta = \kappa^2 \Lambda^2$. As $B \to \infty$, Eqn (88) reduces to the point-like limit (69) and (70).

Figure 3 shows the behavior of $\log_{10}(R/R_N)$ as a function of temperature, calculated using Eqn (88) for $r_0 = 2.3$. The dashed curve represents the solution of Eqn (88) corresponding to the limit $B \to \infty$. It can be seen that the transition becomes broader; however, the qualitative behavior does not change. As discussed above, the behavior of the solution changes qualitatively when r_0 is less than the critical value $r_0^{\rm c} = 1.22$. Figure 4 shows the solution of Eqn (88) for $r_0 = 0.9$, corresponding to the nonpoint-like limit (77).

The S-shaped structure of the $\log_{10}(R/R_N)$ curve is characteristic of a first-order transition. The value of the transition temperature can be calculated by computing the Gibbs free energy $G(T)/k_{\rm B}\Omega$ [107–109] and corresponds to the dashed line in Fig. 4. The transition temperature is $T_{\rm l} = 3.6396$ K, $T_{\rm l} < T_{\rm BKT}$ (vertical line in Fig. 4).

Thus, the basis of the presented consideration is the explicit equations for the density of free vortices and the Gibbs free energy, obtained by applying the ring approximation to handle the long-range vortex–vortex potential (54). In the absence of an external magnetic field, for large core energies, the density of free vortices ϱ is nonzero for all $T \neq 0$; however, one can speak of a Kosterlitz–Thouless-type transition in the sense that ϱ changes very rapidly near the temperature $T_{\rm KT}$. For small core energies, the dissociation of vortex–antivortex pairs occurs via a first-order transition with a transition temperature that depends on the core energy.

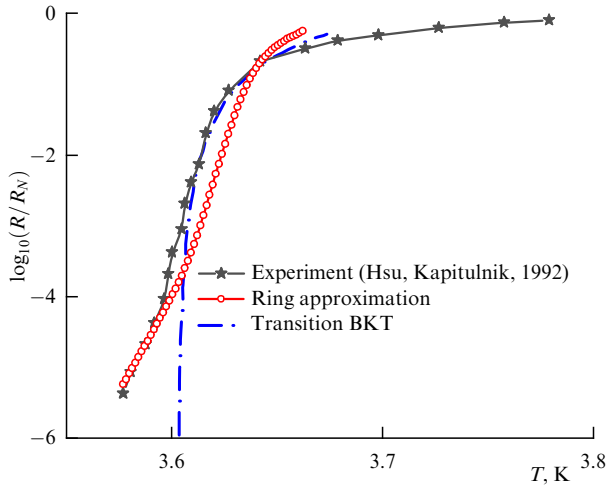

Figure 3. Behavior of $\log_{10}(R/R_N)$ as a function of temperature, calculated using Eqn (88) for $r_0 = 2.3$ (red circles). Black asterisks are experimental points taken from [106]. The dashed line is the fit to BKT behavior [106] obtained using (53) (compare Fig. 1).

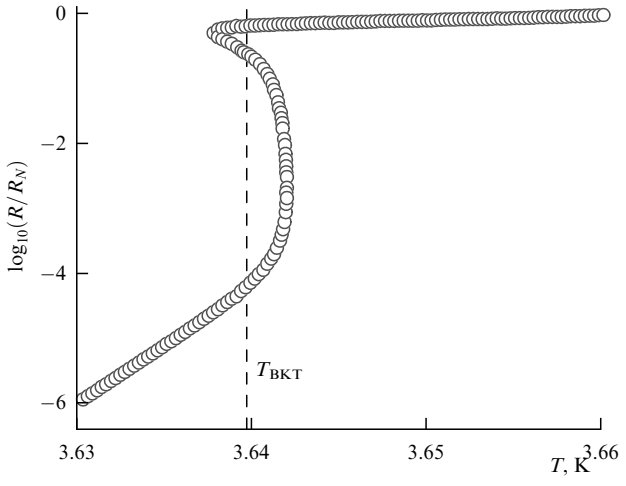

Figure 4. Behavior of $\log_{10}(R/R_N)$ as a function of temperature, calculated using Eqn (88) for $r_0 = 0.9$.

The ring approximation was developed to study the properties of three-dimensional plasma [57, 112]. It was natural to attempt to apply this approximation in the two-dimensional case. In two dimensions, there are two kinds of long-range potentials that are usually encountered: the logarithmic potential, which is the solution of the Poisson equation in two dimensions and is called the two-dimensional Coulomb potential (two-dimensional Coulomb gas [55]), and the ordinary three-dimensional Coulomb potential of the form $1/r$, which is used, for example, to describe a two-dimensional electron system. It can be shown that the application of the ring approximation to the above potentials leads to divergences in the thermodynamic functions: infrared and ultraviolet, respectively. The vortex–vortex interaction potential (54) can be considered as an interpolation between these two potentials, which leads to the fact that in the absence of a magnetic field, the theory presented above is free from divergences.

The experimentally observed transition (see, e.g., Fig. 9 in [106]) is in good qualitative agreement with the obtained results presented in Fig. 3; however, the observed transition is broader. The discrepancy, in our opinion, is explained by the fact that the proposed theory does not take into account pinning, which is always present in experimental samples. The influence of pinning leads to additional dissociation of vortex–antivortex pairs (see, e.g., [94]), which, in turn, should lead to broadening of the curves in Fig. 3.

4. Melting in two dimensions. Scenarios of two-dimensional melting

A separate and very important branch of BKT theory is the theory of two-dimensional melting, developed in the late 1970s in the famous works of Halperin, Nelson, and Young [52–54], in which it was shown that, unlike the case of three dimensions, where melting always occurs via a single first-order transition, in two dimensions the system can melt via two continuous BKT-type transitions. The reason for this is the strongly developed fluctuations in two-dimensional systems. Subsequently, it was found that there exist two other scenarios of two-dimensional melting, which will be discussed in detail below.

Understanding the ordering processes in 2D systems is of great importance for a wide range of various physical fields: photonics and electronics, soft matter physics, the development of new materials, and biotechnology, since knowledge of the phase behavior opens the way to creating systems with desired properties. Despite numerous studies in this direction, fundamental questions remain, related primarily to the dependence of the phase behavior on the specific type of interaction between particles [17, 20, 21, 113].

The study of so-called soft matter, which includes protein solutions, polymers, colloids, dusty plasmas, etc., has to a certain extent revived interest in the statistical mechanics of systems described by fairly simple isotropic effective potentials [20], which are well suited for use within the framework of computer simulation methods. In recent years, a large number of experimental and theoretical (primarily related to the use of computer simulation methods) works devoted to these questions have appeared [114–135, 140, 141, 144, 146–151].

The prediction of the properties of these systems is possible mainly only using effective potentials, which determine the structure of soft matter, its collective dynamics, and thermodynamics. The phase diagrams obtained using effective potentials can qualitatively differ from the case of standard molecular systems such as noble gases. The simplest effective potential that has played a major role in understanding the mechanisms of crystallization and melting of two-dimensional systems is the hard-disk potential [36–39, 136–139, 152–169]; however, even for this potential the results were extremely contradictory, and only recently have works appeared that have brought clarity to this question [154, 155].

For the qualitative description of colloids, polymer globules, and star-shaped polymers, various phenomenological potentials are used, including potentials with negative curvature in the repulsive region (or soft-core potentials) [20, 65–67, 121, 129, 130, 132–135, 170–176, 181–183, 187], bounded potentials such as the Gaussian potential [188–190], or the Hertz potential [20, 21, 177–180, 184–186]. For these systems, the phase diagrams are drastically modified and become more complex compared to the phase diagrams for standard potentials such as the Lennard–Jones potential or hard and soft disks (potential of the form $U(r) = (\varepsilon/r)^{12}$) — a large number of new crystalline phases appear, maxima and

minima on the melting curve, glassy states, as well as anomalous behavior in the liquid phase, which corresponds to well-known water-like anomalies. In this case, in two-dimensional systems, not only various crystalline phases and anomalies in the liquid phase are observed, but also the surprising possibility of observing different melting scenarios in different regions of a single phase diagram.

Two-dimensional melting is observed in a wide variety of physical systems that differ radically from each other in their physical properties and types of interactions — vortex lattices in thin superconducting films [191–201], skyrmion lattices in magnets [202–205], and vortices in Bose–Einstein condensates of ultracold atoms [206].

At the same time, the dependence of the scenarios of two-dimensional melting on the type of potential has not been fully studied even for such a seemingly well-studied system as the Lennard–Jones potential, for which a large number of questions and contradictions remain regarding the melting scenarios and types of phase transitions [207–220].

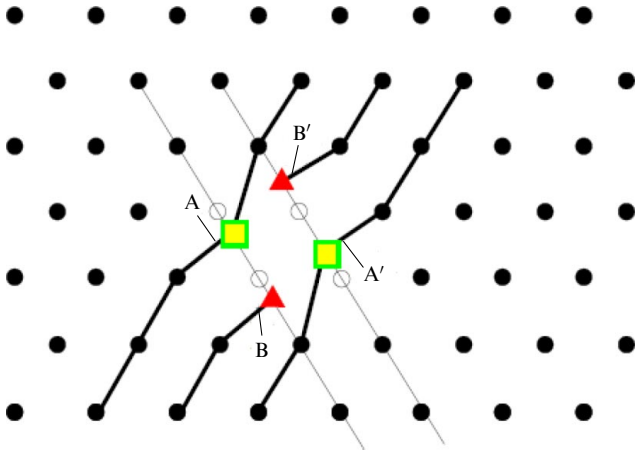

Figure 5. A pair of dislocations, each of which is a disclination dipole. Sites A have 7 nearest neighbors, while B have 5 neighbors.

4.1 The Berezinskii–Kosterlitz–Thouless–Halperin–Nelson–Young (BKTHNY) theory of melting

Even in the original works, Berezinskii [13] and Kosterlitz and Thouless [15] noted that a two-dimensional crystal should melt via the dissociation of dislocation pairs, which in this case are topological defects (Fig. 5). In the presence of quasi-long-range translational order, these defects are well defined. This observation formed the basis of the most popular theory of two-dimensional melting — the Berezinskii–Kosterlitz–Thouless–Halperin–Nelson–Young theory. A crystal lattice is characterized by two types of broken symmetry — translational and rotational, to which two different order parameters correspond and, accordingly, two types of topological defects — dislocations and disclinations, with a dislocation can be represented as a disclination dipole (Fig. 5). The presence of two order parameters and, accordingly, two types of topological defects suggests that the melting of a two-dimensional crystal into an isotropic liquid can occur via two transitions. Let us consider in more detail the melting mechanism underlying the BKTHNY theory.

Quasi-long-range periodic translational order is destroyed by the dissociation of dislocation pairs and the appearance of free dislocations (which play the role of vortices in the X–Y model), which leads to the vanishing of the shear modulus μ. The Hamiltonian describing the system of dislocations in a triangular crystal has the form [17, 52, 54]:

$$H_{\mathrm{dis}} = -\frac{a_0^2 K}{8\pi}\sum_{i\neq j}^{M}\left\{\mathbf{b}(\mathbf{r}_i)\mathbf{b}(\mathbf{r}_j)\ln\frac{r_{ij}}{a} - \frac{\left(\mathbf{b}(\mathbf{r}_i)\mathbf{r}_{ij}\right)\left(\mathbf{b}(\mathbf{r}_i)\mathbf{r}_{ij}\right)}{r_{ij}^2}\right\} + E_{\mathrm{c}}\sum_{i=1}^{M}\mathbf{b}^2(\mathbf{r}_i)\,, \tag{90}$$

where E_{c} is the dislocation core energy, a_0 is the period of the triangular lattice under consideration, $\mathbf{b}$ is the Burgers vector, and the Young's modulus K is given by:

$$K = \frac{4\mu(\mu+\lambda)}{2\mu+\lambda}\,. \tag{91}$$

Here μ and λ are the Lame coefficients [15, 17, 52–54]. The Lame coefficient λ is related to the bulk modulus $B = (\mathrm{d}P/\mathrm{d}\rho)_T = \mu + \lambda$. The Hamiltonian (90) is analogous to the Hamiltonian of the two-dimensional Coulomb gas (12) with the only difference that instead of the scalar 'charge' $q(\mathbf{r})$, a Burgers vector $\mathbf{b}(\mathbf{r})$ appears; therefore, the system described by this Hamiltonian is sometimes called a vector Coulomb gas.

The dissociation of dislocation pairs, leading to melting at temperature T_{m} and being an analog of the dissociation of vortex–antivortex pairs in the standard BKT transition, occurs under the condition [15, 52, 54]:

$$k_{\mathrm{B}}T_{\mathrm{m}} = \frac{Ka_0^2}{16\pi}\,. \tag{92}$$

As in the case of the standard BKT transition, it is necessary to take into account the renormalization of elastic moduli due to bound dislocation pairs. The renormalization-group equations for the Young's modulus of a triangular crystal have the form [53, 54]:

$$\frac{\mathrm{d}K^{*-1}(l)}{\mathrm{d}l} = \frac{3\pi}{4}y^2(l)\exp\left(\frac{K^*(l)}{8\pi}\right)\left(2I_0\left(\frac{K^*(l)}{8\pi}\right) - I_1\left(\frac{K^*(l)}{8\pi}\right)\right), \tag{93}$$

$$\frac{\mathrm{d}y(l)}{\mathrm{d}l} = \left(2 - \frac{K^*(l)}{8\pi}\right)y(l) + 2\pi y^2(l)\exp\left(\frac{K^*(l)}{16\pi}\right)I_0\left(\frac{K^*(l)}{8\pi}\right), \tag{94}$$

where $K^* = a_0^2K/(k_{\mathrm{B}}T)$, l is the scaling variable, and I_0 and I_1 are modified Bessel functions. The infinite-system limit corresponds to $l = \infty$. The unrenormalized Young's modulus K ($l = 0$) and fugacity $y(l=0) = \exp(-E_{\mathrm{c}}/k_{\mathrm{B}}T)$ serve as initial conditions for the system of equations (93) and (94).

The transition temperature T_{m} is given by Eqn (92), in which the renormalization of elastic coefficients due to the presence of bound dislocation pairs in the system, which reduce the system elasticity, is taken into account.

The density–density correlation function $G_T(r)$, which characterizes quasi-long-range translational order, has the form [52, 53]:

$$G_T(r) \propto r^{-\eta_T(T)}\,, \tag{95}$$

where the exponent η_T below the melting temperature T_m takes values

$$\eta_T(T) \leqslant \frac{1}{3}\,. \tag{96}$$

$\eta_T(T_m) = 1/3$ corresponds to the instability of the crystalline phase with respect to the dissociation of dislocation pairs. As in the case of the X–Y model, the heat capacity peak occurs above T_m, with the peak shape depending on the type of system. The inequality (96) plays a fundamentally important role in determining the melting scenario and transition parameters. In this regard, it should be emphasized that relation (96) is *strictly valid only for the melting of a triangular lattice*, which is described by the BKTHNY theory.

At the same time, nontriangular crystal structures have been discovered in computer simulation studies of two-dimensional systems, for example, in systems with two-length-scale potentials [20, 135, 177, 187, 221–225], as well as in water [129, 226]. In works [65–67, 130, 227], the existence of square crystals was shown, and in works [130, 227], a hexagonal structure was also found. The Kagome lattice was found in [121, 129]. A number of publications have reported the possibility of the existence of quasicrystalline structures in two dimensions [187, 228–230]. Exact renormalization-group equations of the type (93) and (94) for nontriangular structures are absent even for the simplest case of a square lattice; in this regard, only an approximate analysis of melting scenarios based on the use of inequality (96) is possible. At the same time, the derivation of the corresponding renormalization-group equations remains a fairly important theoretical task.

Since in a two-dimensional crystal, in addition to quasi-long-range translational order, there exists long-range orientational order, Halperin and Nelson noted [52, 53] that the liquid above the dislocation-pair dissociation point turns out to be nonisotropic. They found that the dissociation of dislocation pairs does not completely destroy the long-range orientational order, but only transforms it into quasi-long-range order [17, 19]. The resulting new phase was called 'hexatic' by analogy with liquid crystals; however, unlike liquid crystals, it is realized in systems with isotropic potentials. Within a fairly rough analogy, the hexatic phase can be represented as an ordered system of hexagonal clusters consisting of a molecule and its six nearest neighbors. In this case, the correlation function of the orientational order parameter for the hexagonal system decays with distance according to a power law (quasi-long-range orientational order). In the hexatic phase, there exist free dislocations; therefore, its shear modulus is zero, i.e., it is a liquid with elements of ordering. A dislocation can be represented as a bound pair of two disclinations (see Fig. 5). The hexatic phase transforms into an ordinary isotropic liquid as a result of the next BKT transition via the dissociation of disclination pairs.

Halperin and Nelson [53] proposed to consider as a phenomenological orientational order parameter for a triangular lattice the quantity:

$$\psi(\mathbf{r}) = \exp\left(6\mathrm{i}\vartheta(\mathbf{r})\right), \tag{97}$$

where $\vartheta(\mathbf{r})$ is the orientation of the bond between two nearest neighbors with respect to some fixed axis. Quasi-long-range order at temperatures above T_m is characterized by a power-law decay of correlations:

$$G_6(r) \propto r^{-\eta_6(T)}\,. \tag{98}$$

To describe long-wavelength fluctuations in an anisotropic liquid, Halperin and Nelson introduced a phenomenological Hamiltonian analogous to the Hamiltonian of the X–Y model [53]:

$$H_A = \frac{1}{2}\,K_A(T)\int \mathrm{d}^2 r\left(\nabla\vartheta(\mathbf{r})\right)^2, \tag{99}$$

where the Frank constant $K_A(T)$ is related to η_6 by the relation:

$$\eta_6(T) = \frac{18 k_B T}{\pi K_A(T)}\,. \tag{100}$$

The dissociation of disclination pairs occurs at $T_i > T_m$. The equation for determining T_i has the form:

$$k_B T_i = \frac{\pi K_A(T_i)}{72}\,, \tag{101}$$

with $\eta_6(T_i) = 1/4$. This value of the exponent corresponds to the temperature of instability of the hexatic phase with respect to the formation of free disclinations, leading to the appearance of an isotropic liquid.

The presented theory is called the Berezinskii–Kosterlitz–Thouless–Halperin–Nelson–Young theory. Within the framework of this theory, a two-dimensional crystal should melt via two continuous BKT-type transitions with an intermediate hexatic phase.

The BKTHNY theory was the most popular for a long time and gave rise to a large number of both experimental and theoretical works based on computer simulations [17], including such exotic systems as vortex systems in thin superconducting films [191–197] and skyrmion lattices [202–205]. At present, relying on both experiment and computer simulations [231], one can state with a sufficient degree of confidence that systems with long-range interactions (e.g., Coulomb or dipole–dipole interactions, soft spheres $1/r^n$ with exponent $n \leqslant 6$) melt in accordance with the BKTHNY scenario.

4.2 Melting of two-dimensional lattices via a first-order transition

At the same time, the standard first-order transition can also be realized. A possible mechanism for a first-order transition caused by the appearance of grain boundaries and the corresponding sharp increase in the number of free dislocations, which occurs prior to the dissociation of dislocation pairs and the corresponding BKT transition, was proposed by S.T. Chui [232] (see also [17, 19, 113]). A grain boundary is a collective excitation of dislocations that is a 'string' of dislocations. The appearance of a grain boundary leads to the rotation of one part of the crystal relative to others. Infinite parallel grain boundaries interact via a short-range potential [113, 232], which leads to the fact that melting occurs according to a scenario different from BKTHNY. The free energies of possible configurations of low-angle grain boundaries were calculated in the low-density approximation of grain boundaries and dislocation pairs, while the renormalization of the dislocation core energy and elastic constants was not considered. As a result, S.T. Chui concluded that prior to the BKTHNY transition, a first-order transition occurs regardless of the magnitude of the dislocation core energy; however, at a core energy $E_c^* > 2.84 k_B T_m$, where T_m is the temperature of dislocation-pair dissociation

(92), the first-order transition becomes close to continuous, but without a hexatic phase. Most likely, S.T. Chui's theory is valid for $E_c < E_c^*$; however, at higher values of the dislocation core energy, the BKTHNY theory is valid. In [233], the so-called coarse-grained Laplace model was studied by Monte Carlo methods, within which it was possible to show that at large values of the dislocation core energy, the BKTHNY scenario takes place, while for $E_c < E_c^*$, a first-order transition occurs.

A crystal can also melt via a single first-order transition in which disclination complexes dissociate and free disclinations appear in the system. A free disclination leads to the rotation of part of the crystal relative to others, which completely destroys both quasi-long-range translational order and orientational order. The Hamiltonian of the system of dislocations and disclinations has the form [19, 234, 235]:

$$\begin{aligned} H_{\text{disl–disc}} = {} & \frac{\pi}{18}\sum_{i\neq j}^{N} s_i s_j \left\{ \frac{K}{8}\, r_{ij}^2 \ln \frac{r_{ij}}{a} \right\} + E_d \sum_{i=1}^{N} s_i^2 \\ & + \frac{a_0 K}{12}\sum_{i=1}^{M}\sum_{j=1}^{N} s_j \epsilon_{mn} b_n(\mathbf{r}_i)(\mathbf{r}_i - \mathbf{r}_j)_m \left(\ln \frac{r_{ij}}{a} + C \right) \\ & - \frac{a_0^2 K}{8\pi}\sum_{i\neq j}^{M} \left\{ \mathbf{b}(\mathbf{r}_i)\mathbf{b}(\mathbf{r}_j) \ln \frac{r_{ij}}{a} - \frac{\left(\mathbf{b}(\mathbf{r}_i)\mathbf{r}_{ij}\right)\left(\mathbf{b}(\mathbf{r}_i)\mathbf{r}_{ij}\right)}{r_{ij}^2} \right\} \\ & + E_c \sum_{i=1}^{M} \mathbf{b}^2(\mathbf{r}_i)\,, \end{aligned} \tag{102}$$

where E_d and E_c are the core energies of disclinations and dislocations, $\mathbf{r}_{ij} = \mathbf{r}_i - \mathbf{r}_j$, and K is given by Eqn (91).

The first two terms describe the energy of interacting disclinations, the third describes the interaction of dislocations with disclinations, and the last two describe the dislocation interaction energy (see (90)). It can be shown that the energy of a given configuration of disclination and dislocation charges is finite only when the following conditions are satisfied:

$$\sum_j s_j = 0, \quad \sum_j \mathbf{r}_j s_j = 0, \quad \sum_j \mathbf{b}(\mathbf{r}_j) = 0\,. \tag{103}$$

Using the Debye–Hückel approximation, it was shown in [17, 19, 234, 235] that melting occurs as a first-order transition at a dislocation core energy $E_c < 2.26$, and in accordance with the BKTHNY scenario at higher core energies, which qualitatively coincides with the result obtained in [232] (see also [113, 233]).

4.3 The Bernard–Krauth (BK) scenario

In 2011, an article by Bernard and Krauth [154] appeared, which was developed in works [142, 155, 231, 236–238], in which the melting of a two-dimensional system of hard disks was considered using computer simulation methods, and another scenario was proposed, according to which the transition from the crystal to the hexatic phase is a continuous BKT-type transition, while the hexatic phase transforms into an isotropic liquid as a result of a first-order transition. The authors proposed a fast Monte Carlo algorithm that was applied to a set of systems with the number of particles ranging from $N = 256^2$ to $N = 1024^2$. The systems under consideration are sufficiently large, and given that extremely long thermalization was applied, one can hope that the obtained results are valid for an equilibrium system in the thermodynamic limit. The proposed scenario received experimental confirmation in [138], in which the behavior of hard colloids confined between transparent plates placed at a slight angle was investigated, which made it possible to simulate the change in local density in the system.

In this regard, the following remark should be made. The study of melting in two-dimensional systems has a long history and began with the original works of Alder and Wainwright [36–39], in which the hard-disk system was considered. In most works, the authors concluded that the melting of this system occurs as a first-order transition [17, 19, 156–166, 168]. At the same time, the work [167] should be mentioned, in which the authors using the Monte Carlo method concluded that the system melts via a single continuous transition without a hexatic phase. Apparently, the reasons for the discrepancies are related to difficulties in achieving true thermodynamic equilibrium and an insufficiently large system size. In this regard, the works of the classic of computer simulation Kurt Binder should be mentioned [166, 239], in the first of which a first-order transition in hard disks was found, while in the second, using molecular simulation and the renormalization-group method, the melting of this system is described as a continuous transition without a hexatic phase. The reason for the contradictions most likely lies in the fact that the system size and simulation time were insufficient to approach the equilibrium thermodynamic limit. It should also be noted that, as shown in [138, 154, 155], the width of the region of existence of the hexatic phase in the hard-disk system is so small that it is difficult to observe against the background of the two-phase region in a first-order transition. We will return to the discussion of this issue in the next section.

Currently, there is no unambiguous and consistent theory of the first-order hexatic-isotropic liquid transition. The likely mechanism is that the BKT transition can become a first-order transition when the core energy of the topological defect decreases [17, 55, 64, 108, 109, 111]; however, a consistent calculation of the disclination core energy is currently absent, which does not allow predicting the nature of the transition depending on the type of intermolecular potential.

At present, relying on both experiment and computer simulations [17, 231], one can state with a sufficient degree of confidence that systems with long-range interactions (e.g., Coulomb or dipole–dipole interactions, soft disks $1/r^n$ with exponent $n \leqslant 6$) melt in accordance with the BKTHNY scenario, while the transition in a system of soft disks with $n > 6$ occurs in accordance with the BK scenario described above.

It should be noted that at present there are no clear theoretical criteria that would make it possible to unambiguously determine, based on the form of the potential, which melting scenario will occur. At the same time, one should take into account the fact that the BKTHNY theory, as well as computer simulations of soft disks [231, 236] and experiments with two-dimensional hard disks [238], pertained to a triangular crystal lattice. However, recently two-dimensional systems with square and more complex lattices have been discovered, to which existing theories can be applied only conditionally when investigating their melting scenarios. Moreover, as discussed in [170, 236, 240], random pinning can alter the melting scenario and transform a first-order transition into two-stage melting with a continuous transition from the crystal to the hexatic phase and a first-order

transition from the hexatic phase to the isotropic liquid. Thus, studying the relationship between the shape of the interparticle potential and the existence of the hexatic phase is an interesting problem that is still far from a definitive solution.

4.4 Determination of two-dimensional melting parameters by computer simulation methods

Several complementary methods are used to determine the boundaries of phase transitions. First of all, the equation of state is calculated. Figure 6a–c) shows the equations of state corresponding to the melting scenarios described above.

In the case of first-order transitions, Mayer–Wood loops should be observed on the equations of state [241] — analogs of van der Waals loops (Fig. 6a), from which the transition boundaries can be determined using the Maxwell construction. The shape of the Mayer–Wood loops depends on the number of particles in the system. As the number of particles increases, the loops become smoother, and in the thermodynamic limit, instead of a loop, a straight line appears, coinciding with the transition line obtained from the Maxwell construction. In principle, Mayer–Wood loops are observed not only in the case of a first-order transition, but also in the case of a standard continuous transition such as the transition in the two-dimensional Ising model [156]; however, the behavior of the loops as the number of particles increases differs in these cases. For a first-order transition, the loop lies in the coexistence region and is due to the interface free energy ΔF. At a given density, the interface free energy, $\Delta f = \Delta F/N$, can be computed by integrating the equation of state [154–156]. In two dimensions, it scales as $\Delta f \propto 1/\sqrt{N}$. In contrast, for a continuous transition, Δf decays faster, so that ΔF is constant, i.e., $\Delta f \propto N^{-1}$, and the equation of state becomes monotonic for sufficiently large system sizes [156]. The scaling of Δf as a function of system size for large system sizes is a reliable indicator of a first-order phase transition [169]. Based on this difference, the authors of the BK scenario argued that they observed a first-order transition. However, this consideration does not take into account the fundamental difference between the transition in the two-dimensional Ising model and the BKT transition.

It should be noted that there is some misunderstanding of the term 'continuous transition' when discussing the behavior of the equation of state in the case of a first-order transition and a continuous transition. To compare the behavior of systems with a first-order transition and a continuous transition, the authors of [156] considered the behavior of the hard-disk system and the Ising model and attempted to apply the results of the study of the transition in the two-dimensional Ising model to interpret the results of computer simulations of two-dimensional melting. In this paper, the behavior of Mayer–Wood loops for the transition in the Ising model and the hard-disk system was analyzed, and the above dependence on the number of particles was obtained. However, the fundamental difference between the second-order transition in the Ising model and the BKT transition was not taken into account. In two spatial dimensions, the Mermin–Wagner theorem strictly shows that in two-dimensional systems with continuous symmetry, long-range order cannot exist at any finite temperature, in contrast to the two-dimensional Ising model. For example, the X–Y model cannot have an ordered phase at low temperature, as in the two-dimensional Ising model. In two-dimensional systems with continuous symmetry, as discussed in the Introduction, there is a continuous BKT transition; however, compared to the continuous second-order transition in the Ising model, the BKT transition is an infinite-order transition, i.e., on both sides of the transition, derivatives of infinite order of the thermodynamic potential are equal to each other, which makes the transition smoother compared to the standard second-order transition [55]. The BKT transition occurs as a result of the dissociation of pairs of topological defects (vortices in the case of the X–Y model, dislocations in the case of the two-dimensional crystal–hexatic transition, and disclinations for the hexatic–isotropic liquid transition). The appearance of a single free topological defect qualitatively changes the behavior of the order parameter correlation function from power-law to exponential decay. In particular, a free dislocation makes the shear modulus of a two-dimensional crystal equal to zero. In this case, there are no phase boundaries that would create Mayer–Wood loops in the case of a second-order transition in a finite system, for example, in the two-dimensional Ising model; therefore, in the case of a BKT transition, a Mayer–Wood loop is impossible altogether. This leads to the fact that for the BKTHNY melting scenario, the equation of state should be monotonic, without any loops and, in principle, almost without a visible bend (see Fig. 6b). As mentioned above, increasing the number of particles in the case of a first-order transition indeed made the loops flatter and slightly changed the size of the two-phase region, but did not eliminate the Mayer–Wood loops [154, 155, 168]. At the same time, in the case of the BKTHNY scenario, changing the number of particles may slightly change the quantitative characteristics of the melting transition, but cannot change the qualitative form of the equation of state.

Equations of state reliably reflect the coexistence region of two phases but do not provide information about the scenario of the transition. To determine the exact boundaries of the hexatic phase and the crystal, one should use an approach based on the long-range behavior of the orientational and translational correlation functions of the order parameters [65–67, 170, 177, 187]. As discussed above (see also [53]), the stability boundary of the hexatic phase can be determined from the condition that the exponent of the orientational correlation function (OCF) $G_6(r)$ (98) is $\eta_6 = 1/4$, while the translational correlation function (TCF) $G_T(r)$ at the crystal–hexatic transition also decays in a power-law manner (107) with an exponent equal to $\eta_T = 1/3$. Figure 6 schematically shows the positions of the stability boundaries for different scenarios. In the case of a first-order transition (see Fig. 6a), these stability boundaries fall inside the two-phase region, while in the case of the BK scenario (Fig. 6c), the stability boundary for the hexatic–isotropic liquid transition falls into the two-phase region, while the BKT transition boundary for the crystal–hexatic transition lies in the stable solid region, which leads to the existence of the hexatic phase.

The region of existence of the hexatic phase is usually rather narrow, which makes its study by computer simulation methods quite difficult. At the same time, in real experiments on two-dimensional melting, the systems under consideration, as a rule, contain random fields of various natures — frozen impurities, random substrate relief, and a random pinning force originating from substrate inhomogeneities.

In the works of Nelson [242, 243], and subsequently in subsequent studies [140, 141, 244–246], it was shown that the introduction of disorder acting on particles should affect the translational and orientational order differently. It is obvious that even a small disorder should strongly disturb the

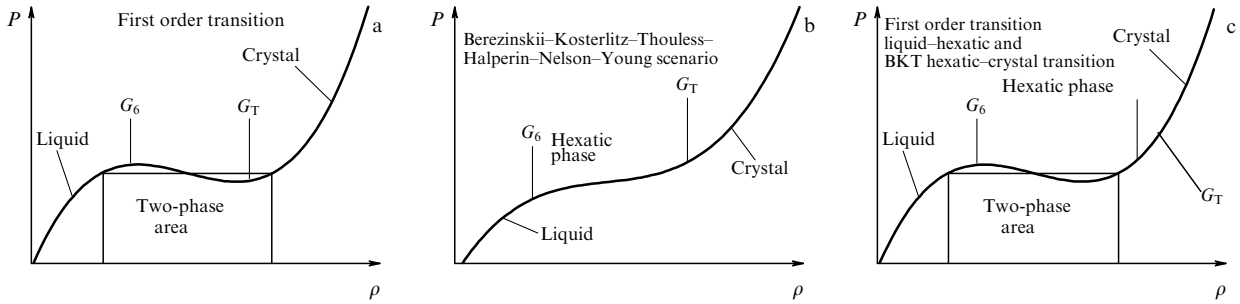

Figure 6. Typical equations of state corresponding to the two-dimensional melting scenarios described in the text. The arrows indicate the stability boundaries of the crystalline and hexatic phases obtained from the analysis of the behavior of the correlation functions of the translational and orientational order parameters. (a) Typical equation of state for a first-order transition. The transition boundaries are determined from the Maxwell construction. (b) Equation of state in the case of the BKTHNY scenario. There are no Mayer–Wood loops on the equation of state. (c) Equation of state corresponding to the BK melting scenario. The boundaries of the hexatic–isotropic liquid transition are determined from the Maxwell construction.

arrangement of particles on lattice sites; at the same time, the orientation of vectors pointing to nearest neighbors should not change significantly due to the presence of point defects. Therefore, translational order should be relatively easily destroyed by disorder, while the effect of disorder on orientational order should be insignificant. As a result, the transition temperature from the crystal to the hexatic phase should decrease, while the transition temperature from the hexatic phase to the isotropic liquid should remain virtually unchanged, which leads to an expansion of the region of existence of the hexatic phase at the expense of the crystal region. In this case, even a situation is possible where a first-order transition is transformed into two transitions in accordance with the BK scenario [170, 186, 240].

The presence of orientational and translational ordering in the system is assessed from the study of the behavior of the corresponding order parameters and their correlation functions.

To assess the degree of orientational ordering, the order parameter of the form

$$\Psi_6(\mathbf{r}_i) = \frac{1}{n(i)} \sum_{j=1}^{n(i)} \exp\left(\mathrm{i}6\theta_{ij}\right), \tag{104}$$

is used, where θ_{ij} is the angle between the vector $\mathbf{r}_{ij}$ connecting the ith and jth particles and an arbitrary axis. The summation is performed over all nearest neighbors of the ith particle $n(i)$. The nearest neighbors are determined by the Voronoi construction.

In addition to the local order parameter $\Psi_6(\mathbf{r_i})$, one can also introduce a global parameter ψ_6, which is the system average of $\Psi_6(\mathbf{r_i})$:

$$\psi_6 = \frac{1}{N} \left\langle \left| \sum_i \Psi_6(\mathbf{r}_i) \right| \right\rangle. \tag{105}$$

Translational ordering in the system is determined from the order parameter

$$\psi_T = \frac{1}{N} \left\langle \left| \sum_i \exp\left(\mathrm{i}\mathbf{G}\mathbf{r}_i\right) \right| \right\rangle, \tag{106}$$

where $\mathbf{r}_i$ is the position vector of the ith particle, and $\mathbf{G}$ is a reciprocal lattice vector.

The translational correlation function has the form:

$$G_T(r) = \frac{\left\langle \exp\left(\mathrm{i}\mathbf{G}(\mathbf{r}_i - \mathbf{r}_j)\right) \right\rangle}{g(r)}, \tag{107}$$

where $r = |\mathbf{r}_i - \mathbf{r}_j|$, and $g(r) = \langle \delta(\mathbf{r}_i)\delta(\mathbf{r}_j) \rangle$ is the radial distribution function. In the crystalline phase without frozen disorder, in the limit $r \to \infty$ $G_T(r) \propto r^{-\eta_T}$, where $\eta_T \leqslant 1/3$ [53].

The orientational correlation function $G_6(r)$ (OCF) is defined in a similar manner:

$$G_6(r) = \frac{\left\langle \Psi_6(\mathbf{r}) \Psi_6^*(\mathbf{0}) \right\rangle}{g(r)}, \tag{108}$$

where $\Psi_6(\mathbf{r})$ is the local orientational order parameter (104). In the hexatic phase, the OCF decays according to a power law: $G_6(r) \propto r^{-\eta_6}$, where $0 \leqslant \eta_6 \leqslant 1/4$ [53]. The hexatic phase loses its stability when the condition $\eta_6(T_\mathrm{i}) = 1/4$ is reached.

In the presence of pinning, we found [170] that the envelope of the TCF in logarithmic coordinates as a function of distance has a kink, after which the criterion of power-law decay of the TCF with an exponent equal to $\eta_T = 1/3$ is applicable for determining the stability boundary of the crystal upon transition to the hexatic phase.

The approaches described above for determining the scenarios and parameters of melting of systems with specific potentials are the most convenient and accurate in the case of studies carried out by computer simulation methods.

4.5 The density functional method in the theory of two-dimensional melting

For further consideration, let us recall the main ideas of the density functional theory for two-dimensional melting [193, 247–251]. As noted above, in the case of two dimensions, due to fluctuations, there is no long-range translational order. Thus, at low temperatures, the local density of the solid, which is proportional to the single-particle distribution function, can be written as a Fourier series over the reciprocal lattice vectors $\mathbf{G}$:

$$\rho(\mathbf{r}) = \sum_{\mathbf{G}} \rho_{\mathbf{G}}(\mathbf{r}) \exp\left(\mathrm{i}\mathbf{G}\mathbf{r}\right), \tag{109}$$

where $\rho_{\mathbf{G}}(\mathbf{r})$ are order parameters for the liquid–solid phase transition. Due to thermal fluctuations, the order parameters $\rho_{\mathbf{G}}(\mathbf{r})$ vary slowly over distances of the order of G^{-1} with amplitude and phase:

$$\rho_{\mathbf{G}}(\mathbf{r}) = \rho_{\mathbf{G}} \exp\left(\mathrm{i}\mathbf{G}\mathbf{u}(\mathbf{r})\right). \tag{110}$$

Here $\mathbf{u}(\mathbf{r})$ denotes the displacement field, which, in general, can be decomposed into a smooth part corresponding to the

phonon field and a singular part that can be interpreted as Berezinskii–Kosterlitz–Thouless vortices [15] and corresponds to dislocations.

Taking into account long-wavelength fluctuations, one can write the Landau expansion in the form [249–251]:

$$\Delta F = \frac{1}{2}\int \mathrm{d}^2 r \sum_{\mathbf{G}} \left[A|\mathbf{G}\times\nabla\rho_{\mathbf{G}}|^2 + B|\mathbf{G}\cdot\nabla\rho_{\mathbf{G}}|^2 + C\,|\rho_{\mathbf{G}}(\mathbf{G}\cdot\nabla)\rho_{\mathbf{G}}|\right] + \frac{1}{2}\,a_T\sum_{\mathbf{G}}|\rho_{\mathbf{G}}|^2 + b_T \sum_{\mathbf{G}_1+\mathbf{G}_2+\mathbf{G}_3=0} \rho_{\mathbf{G}_1}\rho_{\mathbf{G}_2}\rho_{\mathbf{G}_3} + O(\rho^4)\,. \tag{111}$$

ΔF corresponds to the difference in free energies of the crystal and the isotropic liquid. The first term in the expansion (111) has the form of the deformation free energy of a solid. The Lame coefficients μ and λ are functions of the parameters A, B, and C and are proportional to the square of the modulus of the order parameter (109).

Using Eqn (111), the melting scenario in two dimensions can be described as follows. If fluctuations of the order parameter are neglected (exactly as in three dimensions), it follows from Eqn (111) that at some temperature T_{MF} the modulus of the order parameter vanishes via a first-order transition due to the third-order term in the Landau expansion (111). However, there is another possibility: at temperature T_{m}, singular fluctuations of the phase of the order parameter (vortices) appear in the system, which correspond to free dislocations, in accordance with the standard Kosterlitz–Thouless paradigm. In this case, the modulus of the order parameter is nonzero; nevertheless, the system responds to shear without resistance (the shear modulus $\mu = 0$), so the phase above T_{m} can be called a liquid. In fact, this is the hexatic phase with quasi-long-range orientational order [17, 19, 52, 53]. Thus, there are two possibilities: (i) $T_{\mathrm{m}} < T_{\mathrm{MF}}$, then the system melts via two consecutive continuous BKT transitions; (ii) $T_{\mathrm{m}} > T_{\mathrm{MF}}$, then the system melts via a first-order transition.

T_{m} and T_{MF} can be calculated using microscopic expressions for the Helmholtz free energy F of the solid and the elastic moduli [193, 248–251], calculated by considering the asymptotic behavior of correlation functions [252–256]. In this case, the local density of the solid, $\rho(\mathbf{r})$, can be represented as localized Gaussians (width $1/\alpha^{1/2}$) at the lattice sites, i.e., with Fourier components $\rho_{\mathbf{G}} = \rho\exp(-G^2/4\alpha)$, where $\rho = \int \mathrm{d}\mathbf{r}\,\rho(\mathbf{r})/V$ is the average density. We will use the simplest but sufficiently accurate version of the density functional theory [193, 247–252, 255, 257, 258]:

$$\beta\Delta F = \int \mathrm{d}\mathbf{r}\,\rho(\mathbf{r})\,\ln\left[\frac{\rho(\mathbf{r})}{\rho}\right] - \frac{1}{2}\int \mathrm{d}\mathbf{r}\int \mathrm{d}\mathbf{r}'\,c^{(2)}\bigl(|\mathbf{r}-\mathbf{r}'|,\rho\bigr)\bigl[\rho(\mathbf{r})-\rho\bigr]\bigl[\rho(\mathbf{r}')-\rho\bigr], \tag{112}$$

where $c^{(2)}(|\mathbf{r}-\mathbf{r}'|,\rho)$ is the direct correlation function [259], and $\beta = 1/k_{\mathrm{B}}T$. The parameter α is determined from the condition of minimization of the free energy with respect to it. In principle, the parameters of the first-order transition should be determined from relation (112) using the common tangent construction to the free energy curves of the crystal and the isotropic liquid; nevertheless, considering the smallness of the volume jump at the transition, the melting temperature T_{MF} can be obtained with sufficiently high accuracy from the equation $\Delta F = 0$.

The temperature T_{m} can be determined from the BKTHNY criterion [17, 19, 52, 53], which defines the condition under which the crystal lattice becomes unstable due to the appearance of free dislocations.

$$K(T_{\mathrm{m}}) = \frac{a_0^2}{k_{\mathrm{B}}T_{\mathrm{m}}}\frac{4\mu(T_{\mathrm{m}})\bigl(\mu(T_{\mathrm{m}})+\lambda(T_{\mathrm{m}})\bigr)}{2\mu(T_{\mathrm{m}})+\lambda(T_{\mathrm{m}})} = 16\pi\,, \tag{113}$$

where $K(T)$ is Young's modulus, $\mu(T)$ and $\lambda(T)$ are the Lame coefficients, and a_0 is the triangular lattice constant: $a_0^2 = 2/(\sqrt{3}\rho)$.

The expressions for the Lame coefficients have the form [193, 248–251, 256]:

$$\mu = \frac{k_{\mathrm{B}}T}{16\rho}\sum_G \rho_{\mathrm{G}}^2 m_{\mathrm{G}} G^2(\gamma_{\mathrm{G}} + 2\delta_{\mathrm{G}})\,, \tag{114}$$

$$\lambda = \frac{k_{\mathrm{B}}T}{16\rho}\sum_G \rho_{\mathrm{G}}^2 m_{\mathrm{G}} G^2(\gamma_{\mathrm{G}} - 6\delta_{\mathrm{G}}) + k_{\mathrm{B}}T\rho\bigl(1-\rho\tilde{c}^{(2)}(0)\bigr)\,, \tag{115}$$

where

$$\gamma_{\mathrm{G}} = 2\pi\rho\int r^3\,\mathrm{d}r\,c^{(2)}(r;\rho)J_0(Gr)\,,$$

$$\delta_{\mathrm{G}} = 2\pi\rho\int r^3\,\mathrm{d}r\,c^{(2)}(r;\rho)\frac{J_1(Gr)}{(Gr)}\,,$$

$J_0(x)$ and $J_1(x)$ are Bessel functions, m_{G} is the number of reciprocal lattice vectors of the same length, and $\tilde{c}^{(2)}(q)$ is the Fourier transform of the direct correlation function.

For further calculations, an approximate expression for the direct correlation function is needed. In this case, it is convenient to start from the analytical expression for the direct correlation function of hard disks $c_{\mathrm{HD}}^{(2)}(r,\rho)$ [259], obtained in works [257, 258] (see also [249, 250, 260, 261]).

The obtained relations were used to calculate the phase diagrams of a number of two-dimensional systems: the hard-disk system and the $U \propto 1/r$ potential [193, 248, 262], the system with a hard-disk potential to which an attractive well [249, 250] or a repulsive step [251, 256] has been added.

Figure 7 presents the phase diagrams of vortex systems in thin Nb films of thickness 20 nm and 100 nm, calculated using the parameters from [106] (see (75)) and the vortex-vortex interaction potential (54). In the figures, curves (*1*) correspond to the vortex crystal–hexatic vortex phase transition, (*2*) to the transition between the hexatic vortex phase and the vortex liquid, and (*3*) to the upper critical field H_{c2}. It can be seen from the figure that as the film thickness increases, the fluctuation region decreases, while the regions of existence of the hexatic and liquid vortex phases shrink. It should be noted that by the time the cited calculations were performed, no clear phase diagrams of the vortex system had yet been published. At present, one can, for example, refer to the phase diagram of the vortex-system in a thin αMoGe film [198] (Fig. 5 in that article), which qualitatively corresponds to Fig. 7. It should be noted that, to the best of our knowledge, this was the first calculation of the phase diagram of a vortex system based on the full vortex–vortex potential (54).

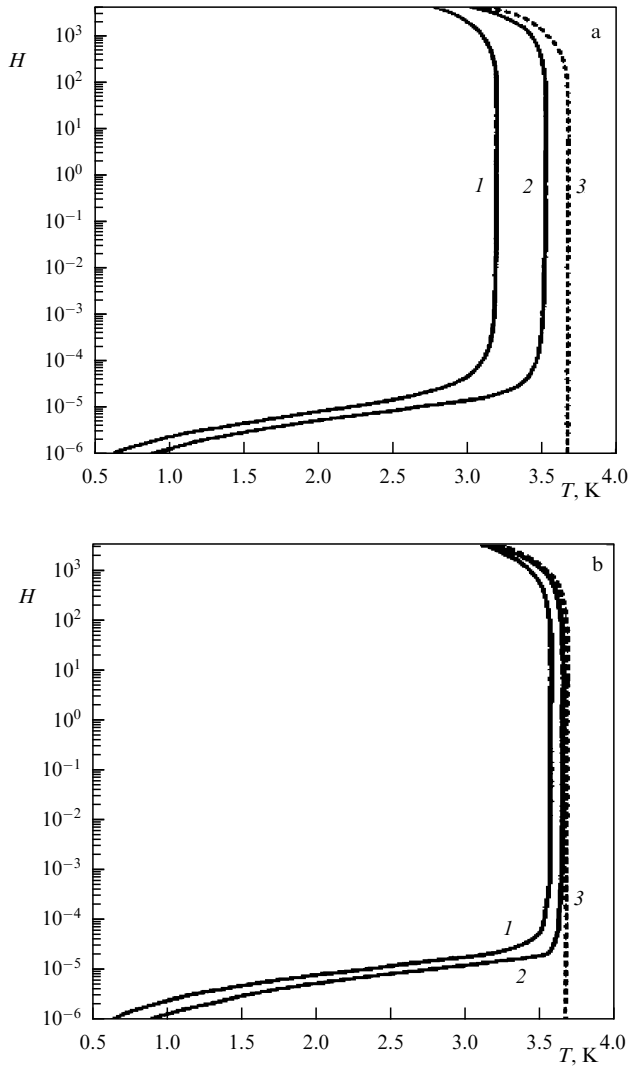

Figure 7. (a) Phase diagram of the vortex system in a niobium film of thickness 20 nm. (b) The same for 100 nm (see [193]). Lines (*1*) correspond to the vortex crystal–hexatic vortex phase transition, (*2*) to the transition between the hexatic vortex phase and the vortex liquid, and (*3*) to the upper critical field H_{c2}.

Within the framework of the density functional method in crystallization theory, it was shown that the melting scenario depends on the type of intermolecular potential [247, 249, 252, 255, 263–268]; however, a detailed description of the dependence of two-dimensional melting scenarios on the type of potential in most cases requires the use of computer simulation methods [17, 19, 20].

5. Conclusion

At present, more than 50 years have passed since the publication of the seminal works of Berezinskii, Kosterlitz, and Thouless, which laid the foundations of a new physics of two-dimensional systems — BKT physics [13–15]. The BKT theory, developed more than 50 years ago, has over time transformed from a rather exotic approach at that time to describing phase transitions in systems where, from the standpoint of the standard theory of that time, no phase transitions should occur at all [18], into a powerful method that has subsequently been extended to a number of physical systems beyond the standard X–Y model and superfluid ^{4}He films, to which the pioneering works [13–15, 43] were primarily devoted. At present, the ideas developed in the original articles of Berezinskii, Kosterlitz, and Thouless are successfully applied to studies of a wide range of various low-dimensional systems, including superconductors and Josephson junction arrays, quasi-two-dimensional systems of ultracold atoms in optomagnetic traps, liquid crystal films, two-dimensional colloids, electrons on the surface of liquid helium, inert gas atoms on substrates (xenon on graphite), two-dimensional granular systems, cylindrical magnetic domains in thin films, vortex systems in high-temperature superconductors and thin superconducting films in a magnetic field, dusty plasmas, thin liquid (water) films, etc. (see, e.g., [16, 17, 19, 22]).

The BKT theory attracted close attention after the appearance of the work of Kosterlitz and Nelson [68] devoted to the superfluid transition in a thin ^{4}He film, and the subsequent brilliant experimental confirmation of this theory [47–49, 69].

Almost simultaneously, the theory of two-dimensional melting developed by Halperin and Nelson [53, 54] appeared (the Berezinskii–Kosterlitz–Thouless–Halperin–Nelson–Young theory), based on the concepts of dissociation of pairs of topological defects (dislocations, disclinations), leading to the destruction of quasi-long-range translational and orientational order via two transitions. The fundamental difference between two-dimensional melting and the case of three dimensions is the possibility that the system should melt via two infinite-order BKT-type transitions with an intermediate orientationally ordered hexatic phase. The BKTHNY theory was for a long time the most popular theory of two-dimensional melting. A characteristic feature of this theory is that the interaction potential does not enter the equations explicitly, which allows this theory to claim universality.

This theory has generated a huge number of experimental and theoretical works. At present, relying on both experiment (see, e.g., [19, 140, 141, 143–150, 269]) and computer simulations [19, 231], one can state with a sufficient degree of confidence that systems with long-range interactions (e.g., Coulomb or dipole–dipole interactions, soft spheres $1/r^n$ with exponent $n \leqslant 6$) melt in accordance with the BKTHNY theory.

At the same time, the situation with the description of two-dimensional melting remains quite controversial. As discussed above, melting can also occur either via a standard first-order transition or in accordance with the Bernard–Krauth scenario, according to which the transition from the crystal to the hexatic phase is a continuous BKTHNY-type transition, while the hexatic phase transforms into an isotropic liquid as a result of a first-order transition. The latter scenario is apparently valid for systems with short-range potentials [19] (for example, in [231], it was shown that in the case of a $1/r^n$ potential, this scenario occurs for $n > 6$). Thus, one can state with a sufficient degree of confidence that the theory of two-dimensional melting only partially corresponds to the canonical BKT theory; in this regard, in computer simulations, it is necessary to follow the methodology described above (see [19]).

At present, there are no clear theoretical criteria that would allow one to unambiguously determine, based on the type of potential, which melting scenario will occur. In early works, the prevailing viewpoint was that systems with short-range potentials melt via a first-order transition, while systems with long-range potentials melt via two continuous transitions with an intermediate hexatic phase in accordance with the BKTHNY theory. However, after the appearance of

works [154, 155, 170, 231, 237], it became clear that the hexatic phase can also exist for short-range potentials, including hard disks. Moreover, as discussed above (see also [170–175]), random pinning can alter the melting scenario and transform a first-order transition into two-stage melting with a continuous transition from the crystal to the hexatic phase and a first-order transition from the hexatic phase to the isotropic liquid. Thus, the study of the relationship between the form of the interparticle potential and the existence of the hexatic phase is an interesting problem that is still far from a definitive solution. Apparently, the first-order transition from the hexatic phase to the isotropic liquid can be explained by the fact that the core energy of the topological defect (disclination) is sufficiently small; however, it is not clear how this energy and the Frank modulus of the hexatic phase are related to the interparticle potential. In general, the problem of calculating the core energy of a topological defect from the interparticle potential remains far from being fully solved.

As already mentioned, the BKTHNY theory was constructed based on the assumption that the crystal structure is triangular. At present, a large number of various types of two-dimensional crystal lattices have appeared, corresponding to different, sometimes quite exotic, potentials. The adaptation of the BKTHNY theory to these structures, the derivation of the corresponding renormalization-group equations, and the derivation of the corresponding stability criteria for crystalline phases also appear to be an important task.

Thin superconducting films provide a very extensive material for studying the possibility of the BKT transition. As discussed above, from the majority of available experimental and theoretical results, one can conclude that BKT physics has been clearly observed in some cases; however, often in the literature, the observation of BKT manifestations has been based on a naive application of the famous canonical BKT formulas. In this case, the long-range behavior of the vortex–vortex interaction potential, as well as the inevitable pinning and the effect of a weak magnetic field on the transition, are not taken into account. This primarily concerns the problem of broadening of the observed transition, which has been attempted to be explained semi-phenomenologically by invoking paraconductivity and phenomenological treatment of pinning. However, as shown above in Section 3.2 [107–111], the use of the full potential within the ring approximation (i.e., going beyond the standard BKT equations) makes it possible to consistently describe the crossover in a superconducting film and significantly improve the qualitative description of the system behavior, in particular, the broadening of the transition. This must be taken into account in order to adopt a sufficiently critical attitude toward manifestations of the BKT transition in experiment.

In conclusion, we would like to emphasize once again that the theory developed more than 50 years ago by Berezinskii, Kosterlitz, and Thouless, for which Kosterlitz and Thouless deservedly received the Nobel Prize in 2016, still remains a powerful stimulus for the study of two-dimensional systems of various natures.

After the review was written, an article [270] appeared in which renormalization-group equations for a square lattice were derived. A fundamental change compared with the exponent for a triangular lattice (96) is that for a square lattice $\eta_T \leqslant 1/4$, which should significantly change the results of calculations of phase diagrams of square lattices.

The work was supported by the Russian Science Foundation grant no. 24-12-00037.

References

1. Landau L D *Zh. Eksp. Teor. Fiz.* **7** 627 (1937); *Phys. Z. Sowjetunion* **11** 545 (1937); *Sobranie Trudov* (Collected Works)Vol. 1 (Moscow: Nauka, 1969) p. 253
2. Patashinskii A Z, Pokrovskii V L *Zh. Eksp. Teor. Fiz.* **46** 994 (1964); *Sov. Phys. JETP* **19** 677 (1964)
3. Patashinskii A Z, Pokrovskii V L *Zh. Eksp. Teor. Fiz.* **50** 439 (1966); *Sov. Phys. JETP* **23** 292 (1966)
4. Kadanoff L P *Physics Physique Fizika* **2** 263 (1966)
5. Fisher M E *Rep. Prog. Phys.* **30** 615 (1967)
6. Wilson K G *Phys. Rev. B* **4** 3174 (1971); *Phys. Rev. B* **4** 3184 (1971)
7. Wilson K G, Fisher M E *Phys. Rev. Lett.* **28** 240 (1972)
8. Wilson K G *Phys. Rev. Lett.* **28** 548 (1972)
9. Patashinskii A Z, Pokrovskii V L *Fluktuatsionnaya Teoriya Fazovykh Perekhodov* (Moscow: Nauka, 1982); Translated into English: *Fluctuation Theory of Phase Transitions* (Oxford: Pergamon Press, 1979)
10. Stanley H E *Introduction to Phase Transitions and Critical Phenomena* (Oxford: Clarendon Press, 1971)
11. Peierls R E *Helv. Phys. Acta* **7** (Suppl. 2) 81 (1934)
12. Peierls R E *Ann. Inst. Henri Poincaré* **5** 177 (1935)
13. Berezinskii V L *Zh. Eksp. Teor. Fiz.* **59** 907 (1970); *Sov. Phys. JETP* **32** 493 (1971)
14. Berezinskii V L *Zh. Eksp. Teor. Fiz.* **61** 1144 (1971); *Sov. Phys. JETP* **34** 610 (1972)
15. Kosterlitz J M, Thouless D J *J. Phys. C* **6** 1181 (1973)
16. Kosterlitz J M *Rep. Prog. Phys.* **79** 026001 (2016)
17. Ryzhov V N, Tareyeva E E, Fomin Yu D, Tsiok E N *Phys. Usp.* **60** 857 (2017); *Usp. Fiz. Nauk* **187** 921 (2017)
18. Ryzhov V N *Phys. Usp.* **60** 114 (2017); *Usp. Fiz. Nauk* **187** 125 (2017)
19. Ryzhov V N, Gaiduk E A, Tareeva E E, Fomin Yu D, Tsiok E N *J. Exp. Theor. Phys.* **137** 125 (2023); *Zh. Eksp. Teor. Fiz.* **164** 143 (2023)
20. Ryzhov V N, Tareyeva E E, Fomin Yu D, Tsiok E N *Phys. Usp.* **63** 417 (2020); *Usp. Fiz. Nauk* **190** 449 (2020)
21. Ryzhov V N, Gaiduk E A, Tareyeva E E, Fomin Yu D, Tsiok E N *Phys. Part. Nucl.* **51** 786 (2020); *Fiz. Elem. Chast. Atom. Yad.* **51** 923 (2020)
22. José J V (Ed.) *40 Years of Berezinskii–Kosterlitz–Thouless Theory* (Singapore: World Scientific, 2013)
23. Landau L D, Lifshitz E M *Statisticheskaya Fizika* Ch. 1 (Moscow: Nauka, 1976); Translated into English: *Statistical Physics* Vol. 1 (Oxford: Pergamon Press, 1980)
24. Bogolubov N N (Jr.) "Kvazisrednie v zadachakh statisticheskoi mekhaniki," in *Sobranie Nauchnykh Trudov v Dvenadtsati Tomakh* (Collection of Scientific Works in Twelve Volumes) Vol. 6 (Moscow: Nauka, 2006) p. 236; Translated into English: "Quasi-averages in problems of statistical mechanics," in *Quantum Statistical Mechanics: Selected Works* (Hackensack, NJ: World Scientific, 2015)
25. Sadovnikov B I, Fedyanin V K *Teor. Mat. Fiz.* **16** 368 (1973); *Theor. Math. Phys.* **16** 901 (1973)
26. Sadovnikov B I, Sorokina E M *Dokl. Akad. Nauk SSSR* **188** 788 (1969); *Sov. Phys. Dokl.* **14** 968 (1970)
27. Mermin N, Wagner H *Phys. Rev. Lett.* **17** 1133 (1966)
28. Mermin N D *Phys. Rev.* **176** 250 (1968)
29. Kagiwada R S et al. *Phys. Rev. Lett.* **22** 338 (1969)
30. Chester M, Yang L C, Stephens J B *Phys. Rev. Lett.* **29** 211 (1972)
31. Henkel R P, Smith E N, Reppy J D *Phys. Rev. Lett.* **23** 1276 (1969)
32. Kukich G, Henkel R P, Reppy J D *Phys. Rev. Lett.* **21** 197 (1968)
33. Clow J R, Reppy J D *Phys. Rev. Lett.* **19** 291 (1967)
34. Amit D J *Phys. Lett. A* **26** 448 (1968)
35. Amit D J *Phys. Lett. A* **26** 466 (1968)
36. Alder B J, Wainwright A W *J. Chem. Phys.* **27** 1208 (1957)
37. Alder B J, Wainwright A W *J. Chem. Phys.* **31** 459 (1959)
38. Alder B J, Wainwright A W *J. Chem. Phys.* **33** 1439 (1960)
39. Alder B J, Wainwright A W *Phys. Rev.* **127** 359 (1962)
40. Stanley H E, Kaplan T A *Phys. Rev. Lett.* **17** 913 (1966)
41. Stanley H E *Phys. Rev. Lett.* **20** 589 (1968)
42. Moore M A *Phys. Rev. Lett.* **23** 861 (1969)
43. Kosterlitz J M, Thouless D J *J. Phys. C* **5** L124 (1972)
44. Kosterlitz J M *J. Phys. C* **7** 1046 (1974)
45. Nagaosa N *Quantum Field Theory in Condensed Matter Physics* (New York: Springer, 1999) DOI:10.1007/978-3-662-03774-4

46. Giamarchi T *Quantum Physics in One Dimension* (Oxford: Oxford Univ. Press, 2004)
47. Bishop D J, Reppy J D *Phys. Rev. Lett.* **40** 1727 (1978)
48. Rudnik I *Phys. Rev. Lett.* **40** 1454 (1978)
49. McQueeney D, Agnolet G, Reppy J D *Phys. Rev. Lett.* **52** 1325 (1984)
50. Hadzibabic Z et al. *Nature* **44** 1118 (2006)
51. Murthy P A et al. *Phys. Rev. Lett.* **115** 010401 (2015)
52. Halperin B I, Nelson D R *Phys. Rev. Lett.* **41** 121 (1978)
53. Nelson D R, Halperin B I *Phys. Rev. B* **19** 2457 (1979)
54. Young A P *Phys. Rev. B* **19** 1855 (1979)
55. Minnhagen P *Rev. Mod. Phys.* **59** 1001 (1987)
56. Young A P *J. Phys. C* **11** L453 (1978)
57. Balescu R *Ravnovesnaya i Neravnovesnaya Statisticheskaya Mekhanika* Vol. 1 (Moscow: Mir, 1978); Translated from English: *Equilibrium and Non-Equilibrium Statistical Mechanics* Vol. 1 (New York: Wiley, 1975)
58. Chaikin P M, Lubensky T C *Principles of Condensed Matter Physics* (Cambridge: Cambridge Univ. Press, 1995)
59. Ohta T *Prog. Theor. Phys.* **60** 968 (1978)
60. Wiegman P B *J. Phys. C* **11** 1583 (1978)
61. Amit D J, Goldschmidt Y Y, Grinstein G *J. Phys. A* **13** 585 (1980)
62. Xu B-W, Zhang Y-M *Phys. Rev. B* **50** 18651 (1994)
63. Ding G-H, Xu B-W *Phys. Rev. B* **51** 12653 (1995)
64. Herbut I *A Modern Approach to Critical Phenomena* (Cambridge: Cambridge Univ. Press, 2007) DOI:10.1017/CBO9780511755521
65. Dudalov D E et al. *J. Phys. Conf. Ser.* **510** 012016 (2014)
66. Dudalov D E et al. *J. Chem. Phys.* **141** 18C522 (2014)
67. Dudalov D E et al. *Soft Matter* **10** 4966 (2014)
68. Nelson D R, Kosterlitz J M *Phys. Rev. Lett.* **39** 1201 (1977)
69. Dash J G *Phys. Rev. Lett.* **41** 1178 (1978)
70. Tung S et al. *Phys. Rev. Lett.* **105** 230408 (2010)
71. Huang C-L et al. *Nature* **470** 236 (2011)
72. Clade P et al. *Phys. Rev. Lett.* **102** 170401 (2009)
73. Rath S P et al. *Phys. Rev. A* **82** 013609 (2010)
74. Pearl J, in *Proc. of the 9th Intern. Conf. on Low Temperature Physics LT-9, 1964* (Eds J G Daunt et al.) (New York: Plenum Press, 1965) p. 566
75. Irz D Y, Ryzhov V N, Tareyeva E E *Phys. Lett. A* **207** 374 (1995)
76. Beasley M R, Mooij J E, Orlando T P *Phys. Rev. Lett.* **42** 1165 (1979)
77. Benfatto L, Castellani C, Giamarchi T "Beresinskii–Kosterlitz–Thouless transition within the sine-Gordon approach: the role of the vortex-core energy," in *40 Years of Berezinskii–Kosterlitz–Thouless Theory* (Ed. J V José) (Singapore: World Scientific, 2013)
78. Sadovskii M V *Quantum Field Theory* 2nd ed. (Berlin: De Gruyter, 2019)
79. Lifshitz E M, Pitaevskii L P *Statisticheskaya Fizika* Ch. 2 *Teoriya Kondensirovannogo Sostoyaniya* (Moscow: Nauka, 1978); Translated into English: *Statistical Physics* Vol. 2 *Theory of the Condensed State* (Oxford: Butterworth-Heinemann, 1980)
80. Sadovskii M V *Statistical Physics* 2nd ed. (Berlin: De Gruyter, 2019)
81. Tinkham M *Introduction to Superconductivity* (New York: McGraw-Hill, 1975)
82. Halperin B I, Nelson D R *J. Low Temp. Phys.* **36** 599 (1979)
83. Zhao W et al. *Solid State Commun.* **165** 59 (2013)
84. Kamlapure A et al. *Appl. Phys. Lett.* **96** 072509 (2010)
85. Mondal M et al. *Phys. Rev. Lett.* **107** 217003 (2011)
86. Sharma M et al. *Nanomaterials* **12** 4109 (2022)
87. Epstein K, Goldman A M, Kadin A M *Phys. Rev. Lett.* **47** 534 (1981)
88. Fiory A T, Hebard A F, Glaberson W I *Phys. Rev. B* **28** 5075 (1983)
89. Venditti G e al. *Phys. Rev. B* **100** 064506 (2019)
90. Benfatto L, Castellani C, Giamarchi T *Phys. Rev. B* **80** 214506 (2009)
91. Baity P G et al. *Phys. Rev. B* **93** 024519 (2016)
92. Doniach S, Huberman B A *Phys. Rev. Lett.* **42** 1169 (1979)
93. Sharma M et al., arXiv:2403.11685
94. Hetel I, Lemberger T R, Randeria M *Nature Phys.* **3** 700 (2007)
95. Yong J et al. *Phys. Rev. B* **85** 180507 (2012)
96. Turneaure S J, Lemberger T R, Graybeal J M *Phys. Rev. B* **63** 174505 (2001)
97. Rüfenacht A et al. *Phys. Rev. Lett.* **96** 227002 (2006)
98. Turneaure S J, Ulm E R, Lemberger T R *J. Appl. Phys.* **79** 4221 (1996)
99. Crane R W et al. *Phys. Rev. B* **75** 094506 (2007)
100. Liu W et al. *Phys. Rev. B* **84** 024511 (2011)
101. Bilbro L S et al. *Nature Phys.* **7** 298 (2011)
102. Jeanneret B et al. *Phys. Rev. B* **40** 11374 (1989)
103. Wallin M *Phys. Rev. B* **41** 6575 (1990)
104. Turneaure S J, Lemberger T R, Graybeal J M *Phys. Rev. Lett.* **84** 987 (2000)
105. Lin Y-H, Nelson J, Goldman A M *Phys. Rev. Lett.* **109** 017002 (2012)
106. Hsu J W P, Kapitulnik A *Phys. Rev. B* **45** 4819 (1992)
107. Hebard A F, Fiory A T *Phys. Rev. Lett.* **50** 1603 (1983)
108. Misra S et al. *Phys. Rev. Lett.* **110** 037002 (2013)
109. Daptary G N et al. *Phys. Rev. B* **94** 085104 (2016)
110. Hetel I, Lemberger T R, Randeria M *Nature Phys.* **3** 700 (2007)
111. Yong J et al. *Phys. Rev. B* **85** 180507 (2012)
112. Baity P G et al. *Phys. Rev. B* **93** 024519 (2016)
113. Bert J A et al. *Phys. Rev. B* **86** 060503 (2012)
114. Caviglia A D et al. *Nature* **456** 624 (2008)
115. Mallik S et al. *Nature Commun.* **13** 4625 (2022)
116. Saito Y et al. *Science* **350** 409 (2015)
117. Arjun H, Chaudhuri P *J. Phys. Condens. Matter* **32** 414001 (2020)
118. Dillmann P, Maret G, Keim P *J. Phys. Condens. Matter* **24** 464118 (2012)
119. Zahn K, Maret G *Phys. Rev. Lett.* **85** 3656 (2000)
120. Khrapak S A *Phys. Rev. Research* **2** 012040 (2020)
121. Piñeros W D, Baldea M, Truskett Th M *J. Chem. Phys.* **145** 054901 (2016)
122. Krebs Z et al. *J. Chem. Phys.* **149** 034503 (2018)
123. Hoang V V, Hieu N T *J. Phys. Chem. C* **120** 18340 (2016)
124. Khrapak S *J. Chem. Phys.* **148** 146101 (2018)
125. Schmidle H e al. *Soft Matter* **8** 1521 (2012)
126. Shankaraiah N, Sengupta S, Menon G I *J. Phys. Condens. Matter* **32** 184003 (2020)
127. Anderson J A et al. *Phys. Rev. X* **7** 021001 (2017)
128. Padilla L A et al. *J. Chem. Phys.* **155** 214901 (2021)
129. Nowack L, Rice S A *J. Chem. Phys.* **151** 244504 (2019)
130. Jain A, Errington J R, Truskett T M *Phys. Rev. X* **4** 031049 (2014)
131. Chen Y et al. *Phys. Rev. Lett.* **127** 018004 (2021)
132. Cardoso D S et al. *Physica A* **566** 125628 (2021)
133. Campos-Villalobos G, Dijkstra M, Patti A *Phys. Rev. Lett.* **126** 158001 (2021)
134. Almudallal A M, Buldyrev S V, Saika-Voivod I *J. Chem. Phys.* **137** 034507 (2012)
135. Rice S A *Chem. Phys. Lett.* **479** 1 (2009)
136. Qi W, Gantapara A P, Dijkstra M *Soft Matter* **10** 5449 (2014)
137. Russo J, Wilding N B *Phys. Rev. Lett.* **119** 115702 (2017)
138. Thorneywork A L et al. *Phys. Rev. Lett.* **118** 158001 (2017)
139. Sampedro Ruiz P, Lei Q, Ni R *Commun. Phys.* **2** 70 (2019)
140. Deutschländer S et al. *Phys. Rev. Lett.* **111** 098301 (2013)
141. Horn T et al. *Phys. Rev. E* **88** 062305 (2013)
142. Qi W, Dijkstra M *Soft Matter* **11** 2852 (2015)
143. Grimes C C, Adams G *Phys. Rev. Lett.* **42** 795 (1979)
144. Gasser U et al. *ChemPhysChem* **11** 963 (2010)
145. Fomin Yu D, Tsiok E N, Ryzhov V N *Phys. Part. Nucl. Lett.* **22** 509 (2025); *Pis'ma Fiz. Elem. Chast. Atom. Yad.* **22** 402 (2025)
146. Keim P, Maret G, von Grünberg H H *Phys. Rev. E* **75** 031402 (2007)
147. von Grünberg H H et al. *Phys. Rev. Lett.* **93** 255703 (2004)
148. Dillmann P, Maret G, Keim P *J. Phys. Condens. Matter* **20** 404216 (2008)
149. Assoud L et al. *Phys. Rev. Lett.* **102** 238301 (2009)
150. Deutschländer S et al. *Phys. Rev. Lett.* **113** 127801 (2014)
151. Vasilieva E V, Petrov O F, Vasiliev M M *Sci. Rep.* **11** 523 (2021)
152. Xu X, Rice S A *Phys. Rev. E* **78** 011602 (2008)
153. Abutbul D, Podolsky D *Phys. Rev. Lett.* **128** 255501 (2022)
154. Bernard E P, Krauth W *Phys. Rev. Lett.* **107** 155704 (2011)
155. Engel M et al. *Phys. Rev. E* **87** 042134 (2013)
156. Alonso J J, Fernandez J F *Phys. Rev. E* **59** 2659 (1999)
157. Zollweg J A, Chester G V *Phys. Rev. B* **46** 11186 (1992)
158. Lee J, Strandburg K J *Phys. Rev. B* **46** 11190 (1992)
159. Weber H, Marx D *Europhys. Lett.* **27** 593 (1994)
160. Allen M P, Frenkel D, Gignac W *J. Chem. Phys.* **78** 4206 (1983)
161. Novaco A D, Shea P A *Phys. Rev. B* **26** 284 (1982)
162. Abraham F F *Phys. Rev. Lett.* **44** 463 (1980)

163. Barker J A, Hendersen D, Abraham F F *Physica A* **106** 226 (1981)
164. Toxvaerd S *Phys. Rev. Lett.* **44** 1002 (1980)
165. Broughton J Q, Gilmer G H, Weeks J D *Phys. Rev. B* **25** 4651 (1982)
166. Weber H, Marx D, Binder K *Phys. Rev. B* **51** 14636 (1995)
167. Fernandez J F, Alonso J J, Stankiewicz J *Phys. Rev. Lett.* **75** 3477 (1995)
168. Mak C H *Phys. Rev. E* **73** 065104 (2006)
169. Lee J, Kosterlitz J M *Phys. Rev. B* **43** 3265 (1991)
170. Tsiok E N et al. *Phys. Rev. E* **92** 032110 (2015)
171. Tsiok E N *Phys. Wave Phenomena* **33** 169 (2025)
172. Tsiok E N et al. *Phys. Part. Nucl. Lett.* **22** 505 (2025); *Pis'ma Fiz. Elem. Chast. Atom. Yad.* **22** (3) 396 (2025)
173. Ryzhov V N, Tareyeva E E, Fomin Yu D, Tsiok E N *Phys. Part. Nucl. Lett.* **22** 501 (2025); *Pis'ma Fiz. Elem. Chast. Atom. Yad.* **22** (3) 391 (2025)
174. Tsiok E N, Bobkov S A, Gaiduk E A, Tareyeva E E, Fomin Yu D, Ryzhov V N *Phys. Wave Phenomena* **32** 171 (2024)
175. Fomin Yu D, Gaiduk Eu A, Tsiok E N, Ryzhov E N *Physica A* **644** 129841 (2024)
176. Fomin Yu D, Tsiok E N, Ryzhov V N *Physica A* **527** 121401 (2019)
177. Fomin Yu D, Gaiduk E A, Tsiok E N, Ryzhov V N *Mol. Phys.* **116** 3258 (2018)
178. Tsiok E N, Gaiduk E A, Fomin Yu D, Ryzhov V N *Soft Matter.* **16** 3962 (2020)
179. Gaiduk Eu A, Fomin Yu D, Tsiok E N Ryzhov V N *Phys. Rev. E* **106** 024602 (2022)
180. Fomin Yu D, Ryzhov V N, Gribova N V *Phys. Rev. E* **81** 061201 (2010)
181. Pàmies J C, Cacciuto A, Frenkel D *J. Chem. Phys.* **131** 044514 (2009)
182. Mandal B K, Mishra P *Mol. Phys.* **118** e1706774 (2020)
183. Miller W L, Cacciuto A *Soft Matter* **7** 7552 (2011)
184. Zu M et al. *Phys. Rev. Lett.* **117** 085702 (2016)
185. Terao T *J. Chem. Phys.* **139** 134501 (2013)
186. Tsiok E N, Fomin Yu D, Gaiduk E A, Ryzhov E A *Phys. Rev. E* **103** 062612 (2021)
187. Kryuchkov N P, Yurchenko S O, Fomin Yu D, Tsiok E N, Ryzhov V N *Soft Matter* **14** 2152 (2018)
188. Mendoza-Coto A et al. *Phys. Rev. B* **109** 064101 (2024); arXiv:2209.02802v1
189. Prestipino S, Saija F, Giaquinta P V *Phys. Rev. Lett.* **106** 235701 (2011)
190. Prestipino S, Saija F *J. Chem. Phys.* **141** 184502 (2014)
191. Roy I et al. *Phys. Rev. Lett.* **122** 047001 (2019)
192. Franz M, Teitel S *Phys. Rev. B* **51** 6551 (1995)
193. Ryzhov V N, Tareyeva E E *J. Exp. Theor. Phys.* **81** 1115 (1995); *Zh. Eksp. Teor. Fiz.* **108** 2044 (1995)
194. Ganguli S C et al. *Phys. Rev. B* **93** 144503 (2016)
195. Guillamon I et al. *Nature Phys.* **5** 651 (2009)
196. Gabay M, Kapitulnik A *Phys. Rev. Lett.* **71** 2138 (1993)
197. Altvater M A et al. *Nano Lett.* **21** 6132 (2021)
198. Roy I et al. *Phys. Rev. Lett.* **122** 047001 (2019)
199. Maccari I et al. *Phys. Rev. B* **107** 014509 (2023)
200. Correa A et al. *Commun. Phys.* **2** 31 (2019)
201. Maccari I et al. *Phys. Rev. Research* **7** 013160 (2025)
202. Garanin D A, Chudnovsky E M *Phys. Rev. B* **107** 014419 (2023)
203. Huang P et al. *Nature Nanotechnol.* **15** 761 (2020)
204. McCray A R C et al. *Nano Lett.* **22** 7804 (2022)
205. Garanin D A, Chudnovsky E M *J. Magn. Magn. Mater.* **606** 172395 (2024)
206. Mithun T et al. *Europhys. Lett.* **123** 20004 (2018)
207. Tsiok E N et al. *J. Chem. Phys.* **156** 114703 (2022)
208. Frenkel D, McTague J P *Phys. Rev. Lett.* **42** 1632 (1979)
209. Toxvaerd S *J. Chem. Phys.* **69** 4750 (1978)
210. Abraham F F *Phys. Rev. Lett.* **44** 463 (1980)
211. Phillips J M, Bruch L W, Murphy R D *J. Chem. Phys.* **75** 5097 (1981)
212. Bakker A F, Bruin C, Hilhorst H J *Phys. Rev. Lett.* **52** 449 (1984)
213. Strandburg K J, Zollweg J A, Chester G V *Phys. Rev. B* **30** 2755 (1984)
214. Hajibabaei A, Kim K S *Phys. Rev. E* **99** 022145 (2019)
215. Li Y-W, Ciamarra M P *Phys. Rev. E* **102** 062101 (2020)
216. Li Y-W, Ciamarra M P *Phys. Rev. Lett.* **124** 218002 (2020)
217. Zhang H et al. *Phys. Rev. E* **89** 062410 (2014)
218. Wierschem K, Manousakis E *Phys. Rev. B* **83** 214108 (2011)
219. Hajibabaei A, Kim K S *Phys. Rev. E* **99** 022145 (2019)
220. Khali S S, Chakraborty D, Chaudhuri D *Soft Matter* **17** 3473 (2021)
221. Leoni F, Franzese G *J. Chem. Phys.* **141** 174501 (2014)
222. Krebs Z et al. *J. Chem. Phys.* **149** 034503 (2018)
223. Tsiok E N, Fomin Yu D, Ryzhov V N *Physica A* **550** 124521 (2020)
224. Padilla L A, Ramírez-Hernández A *J. Phys. Condens. Matter* **32** 275103 (2020)
225. Cardoso D S et al. *Physica A* **566** 125628 (2021)
226. Martelli F et al. *Front. Phys.* **13** 136801 (2018)
227. Marcotte É, Stillinger F H, Torquato S *J. Chem. Phys.* **134** 164105 (2011)
228. Engel M, Trebin H-R *Phys. Rev. Lett.* **98** 225505 (2007)
229. Dotera T, Oshiro T, Ziherl P *Nature* **506** 208 (2014)
230. Pattabhiraman H, Dijkstra M *J. Chem. Phys.* **146** 114901 (2017)
231. Kapfer S C, Krauth W *Phys. Rev. Lett.* **114** 035702 (2015)
232. Chui S T *Phys. Rev. B* **28** 178 (1983)
233. Strandburg K J *Phys. Rev. B* **34** 3536 (1986)
234. Ryzhov V N *Teor. Mat. Fiz.* **88** 449 (1991); *Theor. Math. Phys.* **88** 990 (1991)
235. Ryzhov V N *Zh. Eksp. Teor. Fiz.* **100** 1627 (1991); *Sov. Phys. JETP* **73** 899 (1991)
236. Tsiok E N, Fomin Y D, Ryzhov V N *Physica A* **490** 819 (2018)
237. Qi W, Gantapara A P, Dijkstra M *Soft Matter.* **10** 5449 (2014)
238. Qi W et al. *J. Phys. Condens. Matter* **20** 245102 (2008)
239. Binder K, Sengupta S, Nielaba P *J. Phys. Condens. Matter* **14** 2323 (2002)
240. Gaiduk E A, Fomin Yu D, Tsiok E N, Ryzhov V N *Mol. Phys.* **117** 2910 (2019)
241. Mayer J E, Wood Wm W *J. Chem. Phys.* **42** 4268 (1965)
242. Nelson D R *Phys. Rev. B* **27** 2902 (1983)
243. Sachdev S, Nelson D R *J. Phys. C* **17** 5473 (1984)
244. Dzyubenko A B, Lozovik Yu E *Zh. Eksp. Teor. Fiz.* **102** 284 (1992); *Sov. Phys. JETP* **75** 149 (1992)
245. Cha M-C, Fertig H A *Phys. Rev. Lett.* **74** 4867 (1995)
246. Herrera-Velarde S, von Grünberg H H *Soft Matter* **5** 391 (2009)
247. Ryzhov V N *Teor. Mat. Fiz.* **55** 128 (1983); *Theor. Math. Phys.* **55** 399 (1983)
248. Ryzhov V N, Tareyeva E E *Phys. Rev. B* **51** 8789 (1995)
249. Ryzhov V N, Tareyeva E E *Physica A* **314** 396 (2002)
250. Pomirchi L M, Ryzhov V N, Tareyeva E E *Theor. Math. Phys.* **130** 101 (2002); *Teor. Mat. Fiz.* **130** 119 (2002)
251. Chumakov E S et al. *Physica A* **432** 279 (2015)
252. Ryzhov V N, Tareyeva E E *Phys. Lett. A* **75** 88 (1979)
253. Ryzhov V N, Tareyeva E E *J. Phys. C* **21** 819 (1988)
254. Ryzhov V N *J. Phys. Condens. Matter* **2** 5855 (1990)
255. Ryzhov V N, Tareeva E E *Teor. Mat. Fiz.* **48** 416 (1981); *Theor. Math. Phys.* **48** 835 (1981)
256. Ryzhov V N, Tareeva E E *Teor. Mat. Fiz.* **92** 331 (1992); *Theor. Math. Phys.* **92** 922 (1992)
257. Colot J L, Baus M *Phys. Lett. A* **119** 135 (1986)
258. Baus M, Colot J L *Phys. Rev. A* **36** 3912 (1987)
259. Hansen J P, McDonald I R *Theory of Simple Liquids* (London: Academic Press, 1986)
260. Ryzhov V N, Tareyeva E E, Fomin Yu D *Theor. Math. Phys.* **167** 645 (2011); *Teor. Mat. Fiz.* **167** 284 (2011)
261. Brazhkin V V, Fomin Yu D, Ryzhov V N, Tareyeva E E, Tsiok E N *Phys. Rev. E* **89** 042136 (2014)
262. Ryzhov V N, Tareyeva E E *Physica C* **205** 55 (1993)
263. Fomin Yu D, Mikheyenkov A V, Tsiok E N, Ryzhov V N *J. Chem. Phys.* **163** 224503 (2025)
264. Ryzhov V N, Tareyeva E E *Phys. Lett. A* **158** 321 (1991)
265. Ryzhov V N, Tareyeva E E *Theor. Math. Phys.* **200** 1053 (2019); *Teor. Mat. Fiz.* **200** 147 (2019)
266. Tareyeva E E, Ryzhov V N *Theor. Math. Phys.* **189** 1806 (2016); *Teor. Mat. Fiz.* **189** 464 (2016)
267. Ryzhov V N, Tareyeva E E *Phys. Lett. A* **378** 3567 (2014)
268. Ryzhov V N et al. *Theor. Math. Phys.* **191** 842 (2017); *Teor. Mat. Fiz.* **191** 424 (2017)
269. Brinkman W F, Fisher D S, Moncton D E *Science* **217** 693 (1982)
270. Grampel W, Podolsky D *Phys. Rev. B* **113** 214109 (2026); arXiv:2507.16418